UNIVERSIDADE FEDERAL DO PARANÁ

EDUARDO LUIZ MENOZZO DA ROSA

EVOLUÇÃO DEPOSICIONAL E GLÁCIO-TECTÔNICA DE UM COMPLEXO GERADO EM CONTATO COM O GELO PENSILVANIANO NO SUDESTE DA BACIA DO PARANÁ

CURITIBA

2018

EDUARDO LUIZ MENOZZO DA ROSA

EVOLUÇÃO DEPOSICIONAL E GLÁCIO-TECTÔNICA DE UM COMPLEXO GERADO EM CONTATO COM O GELO PENSILVANIANO NO SUDESTE DA BACIA DO PARANÁ

Dissertação apresentada ao curso de Pós-Graduação em Geologia, Setor de Ciências da Terra, Universidade Federal do Paraná, como requisito parcial à obtenção do título de Mestre em Geologia.

Orientador: Prof. Dr. Fernando Farias Vesely (UFPR)
Coorientador: Prof. Dr. John L. Isbell (UWM)

CURITIBA

2018

FICHA CATALOGRÁFICA ELABORADA PELO SISTEMA DE BIBLIOTECAS/UFPR
BIBLIOTECA DE CIÊNCIA E TECNOLOGIA

R788e Rosa, Eduardo Luiz Menozzo da
Evolução deposicional e glácio-tectônica de um complexo gerado em contato com o gelo pensilvaniano no sudeste da Bacia do Paraná / Eduardo Luiz Menozzo da Rosa. – Curitiba, 2018.
79 p. : il. color. ; 30 cm.

Dissertação - Universidade Federal do Paraná, Setor de Ciências da Terra, Programa de Pós-Graduação em Geologia, 2018.

Orientador: Fernando Farias Vesely.
Coorientador: John L. Isbell.

1. Grupo Itararé. 2. Paleogeografia glacial. 3. Era Glacial Neopaleozoica. I. Universidade Federal do Paraná. II. Vesely, Fernando Farias. III. Isbell, John L. IV. Título.

CDD: 551.72

Bibliotecária: Romilda Santos - CRB-9/1214

MINISTÉRIO DA EDUCAÇÃO
SETOR CIÊNCIAS DA TERRA
UNIVERSIDADE FEDERAL DO PARANÁ
PRÓ-REITORIA DE PESQUISA E PÓS-GRADUAÇÃO
PROGRAMA DE PÓS-GRADUAÇÃO GEOLOGIA

TERMO DE APROVAÇÃO

Os membros da Banca Examinadora designada pelo Colegiado do Programa de Pós-Graduação em GEOLOGIA da Universidade Federal do Paraná foram convocados para realizar a arguição da Dissertação de Mestrado de **EDUARDO LUIZ MENOZZO DA ROSA** intitulada: **EVOLUÇÃO DEPOSICIONAL E GLÁCIO-TECTÔNICA DE UM COMPLEXO GERADO EM CONTATO COM O GELO PENSILVANIANO NO SUDESTE DA BACIA DO PARANÁ**, após terem inquirido o aluno e realizado a avaliação do trabalho, são de parecer pela sua APROVAÇÃO no rito de defesa.

A outorga do título de mestre está sujeita à homologação pelo colegiado, ao atendimento de todas as indicações e correções solicitadas pela banca e ao pleno atendimento das demandas regimentais do Programa de Pós-Graduação.

CURITIBA, 22 de Março de 2018.

FERNANDO FARIAS VESELY
Presidente da Banca Examinadora (UFPR)

CLAUS FALLGATTER
Avaliador Externo (UNISINOS)

CAROLINA DANIELSKI AQUINO
Avaliador Externo (UFPR)

AGRADECIMENTOS

Agradeço primeiramente ao meu grande mestre Prof. Dr. Fernando Farias Vesely por me mostrar os caminhos e as portas a serem abertas durante todo o tempo que estive sob sua orientação. Também por todo o conhecimento compartilhado e pelas oportunidades que me proporcionou.

A todos meus AMIGOS E AMIGAS DE PEDRA que tiver o prazer de desfrutar da companhia desde 2010 quando cheguei em Curitiba e que me acolheram com o maior amor e amizade que alguém pode querer. Juntos podemos escrever uma coleção de vários volumes de histórias bonitas, marcantes e, principalmente, engraçadas que vivemos pelo Brasil afora e dentro da nossa segunda casa, o CEGEP.

Aos meus companheiros de trabalho, integrantes do Laboratório de Análise de Bacias (LABAP), em especial à Prof. Dra. Barbara Trzaskos que, juntamente do Prof. Dr. Fernando Farias Vesely e todos seus orientados, continuam contribuindo para o conhecimento científico das bacias sedimentares brasileiras.

Aos meus fiéis escudeiros de campo Mariposa, Belo, Andreas, Herick e Jun por me auxiliarem durante os maravilhosos dias gélidos e calorosos que passamos juntos na região de São Luiz do Purunã.

Ao pessoal da Mineração Bassani, especialmente ao Jhonny, Baiano e Hamilton (*in memorian*) que deram todo o suporte e nos permitiram erguer os alicerces do Hotel Itararé em sua propriedade, indispensável para o resultado final deste projeto.

A University of Wisconsin-Milwaukee pelo convite e aos companheiros americanos Prof. Dr. John Isbell, Nick Fedorchuk, James Amato e Kathryn Pauls pela amizade, calorosa recepção e hospitalidade em seu país durante a visita de campo realizada.

Agradeço também à Universidade Federal do Paraná, por todo o suporte e dinheiro investido na minha formação desde meu ingresso em 2010 e por ser a instituição que me ajudou a realizar muitos sonhos e objetivos na vida.

A CAPES e CNPq pela verba investida para a realização do presente projeto através da bolsa de estudos concedida e financiamento através do projeto “Depósitos de transporte em massa na sucessão neopaleozoica na Bacia do Paraná: estratigrafia, aspectos estruturais e significado tectônico”.

Aos meus queridos pais, Sidney e Fabiane, ao meu irmão Arthur e a todos meus familiares, grandes professores da vida que me deram o melhor suporte e apoio possível na minha formação profissional e como pessoa.

E por fim, gostaria de agradecer ao fantástico e dinâmico planeta Terra, gerado dentre inúmeras possibilidades e berço da deslumbrante vida que até hoje conhecemos, pela oportunidade de poder estudá-lo e dizer a todos com muito orgulho que sou Geólogo!

RESUMO

Ambientes de sedimentação relacionados diretamente à ação glacial estão entre os sítios deposicionais mais complexos conhecidos devido aos impactos das sucessivas flutuações da margem da geleira no acúmulo, erosão e deformação da pilha sedimentar. Aliado a este fator, a carência de estudos e entendimento dos processos envolvidos na geração destes depósitos é condicionada pela escassez no registro geológico pré-pleistocênico, uma vez que depósitos glaciais *stricto sensu* são raros no registro estratigráfico. Depósitos gerados nestas condições desempenham um papel fundamental em reconstruções paleogeográficas em bacias sedimentares glaciadas, bem como no entendimento da dinâmica de geleiras pretéritas e de variações climáticas no passado da Terra. Visando contribuir para o entendimento da Era Glacial Neopaleozoica na Bacia do Paraná e, considerando que a análise combinada de fácies sedimentares e estruturas erosivas e deformacionais glaciogênicas é uma importante abordagem para realizar inferências sobre a dinâmica de paleogeleiras, o presente trabalho apresenta uma caracterização em detalhe de um complexo em contato com o gelo situado na base do Grupo Itararé na borda leste da Bacia do Paraná. A sucessão em questão possui até 80 m de espessura e registra a ocorrência de três ciclos de avanço e recuo de três diferentes lobos glaciais ativos durante o máximo glacial da Era Glacial Neopaleozoica. O primeiro ciclo glacial está registrado em um corpo tabular de diamictito maciço compreendido entre superfícies estriadas subglaciais que registram um avanço glacial para N. O segundo ciclo glacial compreende dois ciclos de menor magnitude relacionados a um lobo glacial que avançou para SSW. Estes ciclos estão materializados em depósitos gerados nas zonas pró-glacial e glácio-marginal deformados em diferentes posições e momentos devido à menores flutuações da margem da geleira. Embasada por uma discordância, a espessa sucessão areno-cascalhosa, depositada em contexto glácio-marginal e sotoposta a um espesso tillito subglacial, registra a ação do terceiro ciclo glacial e a transição de uma deformação glácio-marginal para subglacial resultante de um lobo glacial que avançou para NW. A definição destes três ciclos glaciais indica que o cenário paleogeográfico da região é mais complexo do que previamente hipotetizado e que a análise em detalhe de sucessões que registrem a ação glacial direta é fundamental na análise da paleogeografia da Era Glacial Neopaleozoica.

Palavras-chave: Grupo Itararé, paleogeografia glacial, Era Glacial Neopaleozoica.

ABSTRACT

Styles of glaciation and timing of Late Paleozoic Ice Age (LPIA) glaciers are still under debate. In Paraná Basin, ice-contact deposits are rarely exposed due to its low degree of preservation and because of their capping by thick glaciomarine deglaciation sequences that comprise the bulk of the sediment fill in this basin. In this paper, we present new glaciodynamic and paleo-ice flow interpretations for a Lower Pennsylvanian ice-contact complex in the lowermost Itararé Group (Lagoa Azul Formation), Paraná State, southern Brazil. The research was conducted by combining the analysis of contemporaneous glacial facies associations, erosive landforms and glaciotectonic structures. The 80 m-thick ice-contact complex rest over the Itararé Group basal nonconformity and comprises four stacked informal stratigraphic units regarded as the depositional/deformational record of three high-frequency cycles of ice lobes advance/retreat. Glacial cycle 1 (GC1) comprises a sheet of massive and sheared, clast-rich, sandy tillite resting on striated pavements carved in Devonian sandstones and topped by grooved/fluted surfaces indicating a northward flowing ice lobe. Glacial cycle 2 (GC2) is a major cycle that shows a westward-southwestward kinematics of a grounded ice lobe with minor ice-margin fluctuations. It is recorded in a lower subglacially to ice-marginally deformed assemblage deposited in a proglacial marine setting overlaid by a succession deposited in proximal to distal settings of a grounding-line system subsequently deformed in an ice-marginal setting due to renew ice push. Floored by an unconformity, glacial cycle 3 (GC3) is materialized by a thick overridden push-moraine composed of grounding-line fan deposits and capped by a muddy tillite. It records an upward transition from ice-marginal to subglacial deformation by an ice lobe advancing to the northwest. The examined ice-contact complex is interpreted to be a result of multiple advances of, at least, two different ice lobes nucleated in the Windhoek Highlands in Namibia. This stratigraphic interval elucidates the interaction of different glaciers in a relatively short time period during the maximum development of LPIA glaciation and indicates different patterns of ice-flow during the LPIA onset in the eastern margin of the Paraná Basin.

Keywords: Itararé Group, glacial paleogeography, Late Paleozoic Ice Age

LISTA DE FIGURAS

LISTA DE TABELAS

SUMÁRIO

1 INTRODUÇÃO

Ambientes glaciais de sedimentação possuem ampla distribuição geográfica e temporal e são relacionados principalmente a períodos de significativa diminuição da temperatura global (*icehouse Earth*). Desde as primeiras observações e discussões, no século XVIII, acerca da existência de períodos glaciais pretéritos, muito têm se hipotetizado sobre os fatores que influenciaram o decréscimo da temperatura na superfície da Terra, bem como a influência que as massas de gelo exerceram sobre a dinâmica das bacias sedimentares e variações globais no nível do mar (Flint 1957, Veevers and Powell 1987, Crowell 1999). Evidências que registram a presença de ambientes glaciados e eras glaciais são documentadas tanto em ambientes modernos (Atkins *et al.* 2002, Kjaer *et al.* 2008), assim como durante o Cenozoico (Attig *et al.* 1989, Syverson and Colgan 2004, Arzhannikov *et al.* 2012, Urban and Bigga 2015), Mesozoico (Frakes and Francis 1988, Crowell 1999), Paleozoico (Caputo and Crowell 1985, Hambrey 1985, Visser 1987, Le Heron *et al.* 2009, Bussert 2014, Limarino *et al.* 2014), Proterozoico (Lindsey 1971, Chumakov 1981) e Arqueano (Young *et al.* 1998).

Os eventos de recuo e avanço de geleiras sucedidos durante as eras glaciais conhecidas são documentados no registro estratigráfico: 1) diretamente, através de feições erosivas, deformacionais e fácies sedimentares glaciais *stricto sensu* e 2) indiretamente, através da ciclicidade deposicional de sucessões marinhas glácio-influenciadas que contêm evidências da ação glacial (e.g. lamitos com clastos caídos, depósitos de transporte de massa contendo clastos estriados e facetados.

A análise do registro glacial *stricto sensu* se faz difícil em razão do baixo potencial de preservação de fácies e estruturas erosivas geradas em contexto subglacial e glácio-marginal, visto que as flutuações das margens glaciais impactam diretamente no acúmulo, erosão e deformação da pilha sedimentar. Aliado a este fator, a carência de estudos em detalhe dos processos envolvidos na geração destes depósitos é condicionada pela

escassez no registro geológico glaciogênico pré-pleistocênico, uma vez que estes depósitos contribuem com uma parcela ínfima no registro estratigráfico glacial quando comparados aos depósitos marinhos glácio-influenciados, estes melhor preservados e detalhados.

Fácies sedimentares, estruturas erosivas e deformacionais geradas em contexto subglacial e glácio-marginal são de suma importância na reconstrução da paleogeografia de eras glaciais em razão de testemunharem as flutuações de antigas margens glaciais, fornecendo subsídios para a reconstrução de variações climáticas no passado da Terra, bem como para o entendimento paleoglaciológico e da dinâmica glacial pretérita (Bennett and Glasser 2009).

Na Bacia do Paraná, desde as primeiras observações acerca do registro da ação glacial da Era Glacial Neopaleozoica (White 1908, du Toit 1927, Carvalho 1940), diversos trabalhos vêm sendo realizados em todas as porções do Grupo Itararé buscando a melhor caracterização deste período glacial na bacia. A maior parte destes trabalhos tem como foco a análise da arquitetura deposicional e definição de ciclos e ambientes de sedimentação de sucessões essencialmente marinhas depositadas sob influência indireta das geleiras (e.g. Schneider *et al.* 1974, França and Potter 1988, Canuto 1993, Vesely and Assine 2004, d'ávila 2009). Entretanto, trabalhos também vêm sendo realizados visando a caracterização de raras fácies e estruturas erosivas e deformacionais glaciogênicas com a finalidade de aprimorar o entendimento sobre a dinâmica das massas de gelo neopaleozoicas (e.g. Almeida 1948, Bigarella *et al.* 1967, Rocha-Campos *et al.* 1976, Gesicki *et al.* 2002, Vesely *et al.* 2015, Fallgatter and Paim 2017).

Tendo em vista a importância das informações passíveis de serem extraídas a partir da análise do registro glaciogênico, o presente trabalho consiste na caracterização detalhada de um complexo em contato com o gelo, previamente documentado por Vesely *et al.* (2015), situado espacialmente na porção sudeste do estado do Paraná e

estratigraficamente na base do Grupo Itararé (Formação Lagoa Azul; França and Potter 1988). Sendo assim, os resultados e discussões serão apresentados na forma do artigo intitulado "*Constraining the ice-kinematics and glacial cyclicity during the Late Paleozoic Ice Age onset in eastern Paraná Basin*", o qual será submetido ao periódico *Sedimentary Geology*.

2 MÉTODOS DE TRABALHO

2.1 ÁREA DE ESTUDO E AQUISIÇÃO DOS DADOS

Visando a caracterização do intervalo e o mapeamento de fácies e feições glaciogênicas foi conduzido trabalho de campo dividido em três campanhas, totalizando 32 dias. Foram examinadas 44 exposições onde aflora o intervalo de interesse, as quais consistem em afloramentos naturais, cortes em rodovias e ferrovias e cavas de explotação de areia (Tabela 1). O intevalo estratigráfico glaciogênico em questão se encontra distribuído ao longo da porção sul da Escarpa de São Luiz do Purunã, na região dos municípios de Balsa Nova e Palmeira (ver Fig. 2).

Tabela 1 - Afloramentos estudados com suas respectivas coordenadas (UTM) e correlação com as localidades apresentadas na Figura 2.

Ponto	UTM		Ponto (Fig. 2)	Ponto	UTM		Ponto (Fig. 2)
	X	Y			X	Y	
1	635070	7162883	1	23	628975	7174737	11
2	634941	7164953		24	631950	7175555	
3	634751	7166004		25	630133	7177096	12
4	635286	7165726		26	633832	7177338	
5	630499	7168169	2	27	633578	7177516	13
6	628089	7167481	3	28	633650	7178299	13
7	627254	7167174	4	29	634029	7178651	13
8	626952	7167045	4	30	633490	7179883	
9	626198	7168026	5	31	634055	7180466	14
10	626204	7168423	5	32	634094	7180576	
11	626377	7169258	6	33	634020	7180816	
12	626192	7169786	7	34	634305	7180972	
13	625890	7170091	7	35	634142	7181167	
14	624486	7170207		36	634406	7181362	
15	623583	7170371	8	37	631729	7182190	15
16	622904	7170829	9	38	630978	7182107	
17	622570	7171075		39	629495	7181693	16
18	621962	7171432	10	40	629248	7181515	16
19	633156	7171570		41	618803	7187567	17
20	630192	7172880		42	618488	7187761	18
21	630055	7174331	11	43	617232	7189407	
22	629351	7174776	11	44	615085	7189464	19

2.2 ANÁLISE ESTRATIGRÁFICA

A fim de definir e classificar fácies sedimentares, foi utilizada a classificação de litotipos clásticos de Hambrey and Glasser (2012) (Tabela 2). Nesta classificação os litotipos são classificados de acordo com a razão areia/lama na matriz e porcentagem de cascalho no arcabouço. A escolha desta classificação se deve ao fato desta ter sido desenvolvida com base no estudo de geleiras modernas e se enquadra melhor nas variáveis do objeto de estudo, o qual é constituído por uma ampla gama de litotipos mal selecionados.

Tabela 2 – Classificação não-genética de sedimentos e equivalentes litificados utilizada neste projeto (Hambrey and Glasser 2012).

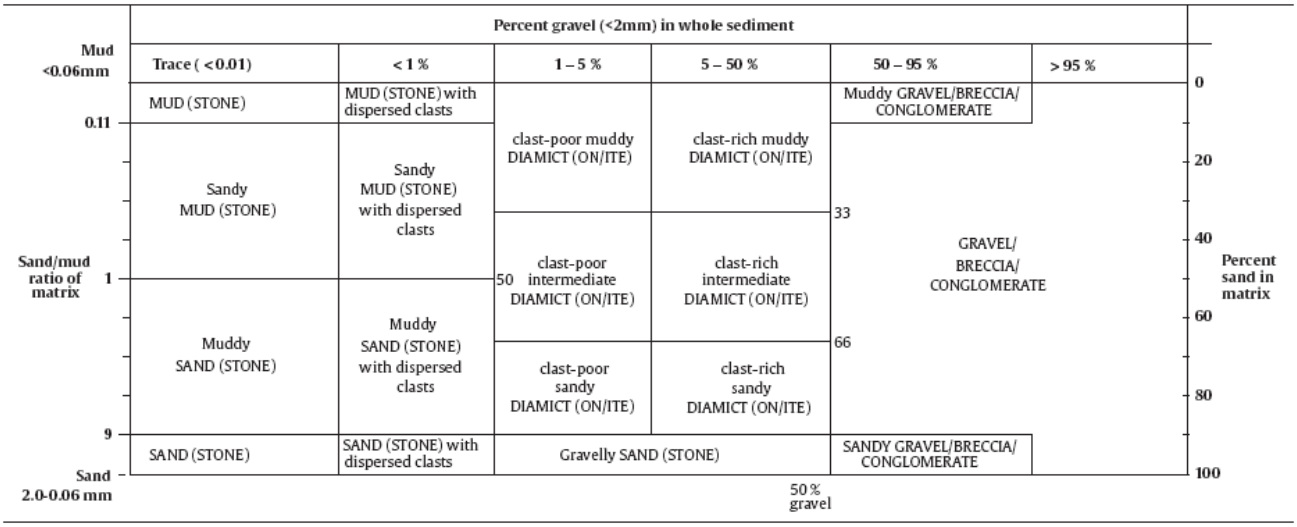

Com base na geometria e relações espaciais das 14 litofácies descritas foi possível interpretar processos deposicionais e deformacionais e identificar três associações de fácies referentes à diferentes zonas no ambiente glacial (subglacial, glácio-marginal e pró-glacial). O discernimento dos processos relacionados à gênese das fácies, juntamente com a análise de associações de fácies e correlação dos empilhamentos verticais levantados permitiu o reconhecimento de sistemas deposicionais e suas relações com flutuações da margem da geleira.

Um dos métodos empregados no reconhecimento de fácies, associações de fácies e do empilhamento estratigráfico regional foi o levantamento de seis perfis sedimentológicos

na escala 1:50. A correlação dos perfis a partir da topografia é impraticável na região dado que eventos tectônicos pós-deposicionais (reativações fanerozoicas da Falha da Lancinha e soerguimento Mesozoico do Arco de Ponta Grossa) resultaram na alteração da estratigrafia original, sendo assim a correlação foi feita pela discordância angular basal sobre os arenitos devonianos da Formação Furnas.

2.3 ANÁLISE DE PALEOCORRENTES E PALEOFLUXO GLACIAL

A definição da polaridade do preenchimento sedimentar e dos sentidos de fluxo dos lobos glaciais que conferem a assinatura glacial para o intervalo foi realizada através da:

- Análise de paleocorrentes em diagramas de roseta sinópticos contendo as mensurações de cada unidade aqui definida. As 705 paleocorrentes foram aferidas em depósitos gerados por fluxo trativo unidirecional gerados nas zonas glácio-mmarginal e pró-glacial, tais como estratificações cruzadas tabulares e acanaladas presentes em arenitos e conglomerados e; marcas onduladas assimétricas e marcas onduladas assimétricas cavalgantes em arenitos;
- Análise da orientação de sulcos, estrias, cristas, *flutes* e sulcos em crescentes contidos em sete superfícies geradas em contexto subglacial;
- Análise da orientação de estruturas deformacionais penecontemporâneas impressas em sedimentos inconsolidados e relacionadas ao cisalhamento imposto por geleiras durante fases de avanço. Foram aferidas um total de 1193 estruturas glácio-tectônicas que compreendem planos de acamamento dobrados, planos/superfícies de cisalhamento, planos de cavalgamento e *slickensides.* As estruturas identificadas foram tratadas estatisticamente através de diagramas estereográficos pelo software OpenStereo. A vergência da deformação indicada pelas estruturas presentes e

relacionada ao sentido de paleofluxo glacial para cada unidade foi obtida através do polo máximo obtido para cada estereograma.

2.4 ANÁLISE DE FOTOMOSAICOS

Algumas exposições nas áreas de estudo (cavas de explotação de areia e cortes em ferrovia) contam com boa continuidade lateral e vertical. Isto possibilitou a construção de fotomosaicos como recurso auxiliar pretendendo a melhor visualização da disposição dos estratos, assim como suas continuidades laterais e estilos de deformação impostos. Sobre as imagens construídas, foram traçadas superfícies limitantes de estratos, bem como estruturas glácio-tectônicas, visando delinear a arquitetura deposicional e deformacional.

3 CONSTRAINING THE ICE-KINEMATICS AND GLACIAL CYCLICITY DURING THE LATE PALEOZOIC ICE AGE ONSET IN EASTERN PARANÁ BASIN

Abstract

Styles of glaciation and timing of Late Paleozoic Ice Age (LPIA) glaciers are still under debate. In Paraná Basin, ice-contact deposits are rarely exposed due to its low degree of preservation and because of their capping by thick glaciomarine deglaciation sequences that comprise the bulk of the sediment fill in this basin. In this paper, we present new glaciodynamic and paleo-ice flow interpretations for a Lower Pennsylvanian ice-contact complex in the lowermost Itararé Group (Lagoa Azul Formation), Paraná State, southern Brazil. The research was conducted by combining the analysis of contemporaneous glacial facies associations, erosive landforms and glaciotectonic structures. The 80 m-thick ice-contact complex rest over the Itararé Group basal nonconformity and comprises four stacked informal stratigraphic units regarded as the depositional/deformational record of three high-frequency cycles of ice lobes advance/retreat. Glacial cycle 1 (GC1) comprises a sheet of massive and sheared, clast-rich, sandy tillite resting on striated pavements carved in Devonian sandstones and topped by grooved/fluted surfaces indicating a northward flowing ice lobe. Glacial cycle 2 (GC2) is a major cycle that shows a westward-southwestward kinematics of a grounded ice lobe with minor ice-margin fluctuations. It is recorded in a lower subglacially to ice-marginally deformed assemblage deposited in a proglacial marine setting overlaid by a succession deposited in proximal to distal settings of a grounding-line system subsequently deformed in an ice-marginal setting due to renew ice push. Floored by an unconformity, glacial cycle 3 (GC3) is materialized by a thick overridden push-moraine composed of grounding-line fan deposits and capped by a muddy tillite. It records an upward transition from ice-marginal to subglacial deformation by an ice lobe advancing to the northwest. The examined ice-contact complex is interpreted to be a result of multiple advances of, at least, two different ice lobes nucleated in the Windhoek Highlands in Namibia. This stratigraphic interval elucidates the interaction of different glaciers in a relatively short time period during the maximum development of LPIA glaciation and indicates different patterns of ice-flow during the LPIA onset in the eastern margin of the Paraná Basin.

Keywords: Itararé Group, glacial paleogeography, glaciotectonics, subglacial, push-moraine, grounding-line fan

3.1 INTRODUCTION

Former ice ages are documented in the stratigraphic record by erosional, depositional and deformational products formed directly or indirectly by glaciers, such as erosive landforms, subglacial tillites and glaciotectonized facies, as well successions comprising outwash deposits, ice-rafted debris and resedimented glacial material (Flint 1957, Frakes 1979, Crowell 1999). The Late Paleozoic Ice Age (LPIA) is one of the best understood former glacial periods and its sedimentary record is widespread in former mid- to high-paleolatitude sedimentary basins of Gondwana (Sen 1980, Santos *et al.* 1996, Visser 1997, Isbell *et al.* 2003, Fielding *et al.* 2008, Bussert 2014, Limarino *et al.* 2014).

Nevertheless, the LPIA record is mostly composed of marine glacially-influenced deposits whereas sedimentary products, erosional and deformational features emplaced directly by glaciers are rarely recognized in the stratigraphic record (e.g. Almeida 1948, Braakman *et al.* 1982, Starck *et al.* 1993, Campos and Dardenne 2002, Le Heron 2017). Due to post-depositional weathering and tectonics, and a thick deglacial sedimentary cover, the glacial landsystems geomorphological approach widely used to high-resolution reconstructions of former glaciers in the Cenozoic Ice Age (Evans *et al.* 1999, Evans 2005, Ottesen *et al.* 2016, Darvill *et al.* 2017) is difficult to apply in the LPIA record, precluding detailed paleoglaciologic and paleogeographic reconstructions.

Subglacial erosive landforms mainly placed on the LPIA deposits basal nonconformity are the most reliable and widely used elements concerning the LPIA glaciers kinematics and basal thermal regime (e.g. Visser 1987, Bussert 2010, Rosa *et al.* 2016). Moreover, the spatial orientation of glaciotectonic structures developed at subglacial and ice-marginal zones, even if rarely described and discreetly used in the LPIA record (Isbell 2010, Rocha-Campos *et al*. 2000, Henry *et al*. 2012, Aquino *et al*. 2016), consists in a powerful tool to determine the glacier kinematics and glacial cyclicity in between pre-Pleistocene strata, as testified on Cenozoic glaciated regions (e.g. Berthelsen 1978,

Huddart and Hambrey 1996, Hart and Watts 1997, Boulton *et al.* 1999, Benn and Clapperton 2000, Henriksen *et al.* 2001).

The intracratonic Paraná Basin of southwestern Gondwana comprises the thickest (up to 1300 m) LPIA record, which is contained in the late Bashkirian to early Sakmarian Itararé Group (Fig. 1A) and its chronologically correlated units located in other margins of the basin (Aquidauana, San Gregório, Coronel Oviedo and Aquidabán formations; Rocha-Campos and Santos 1981, Fúlfaro 1996).

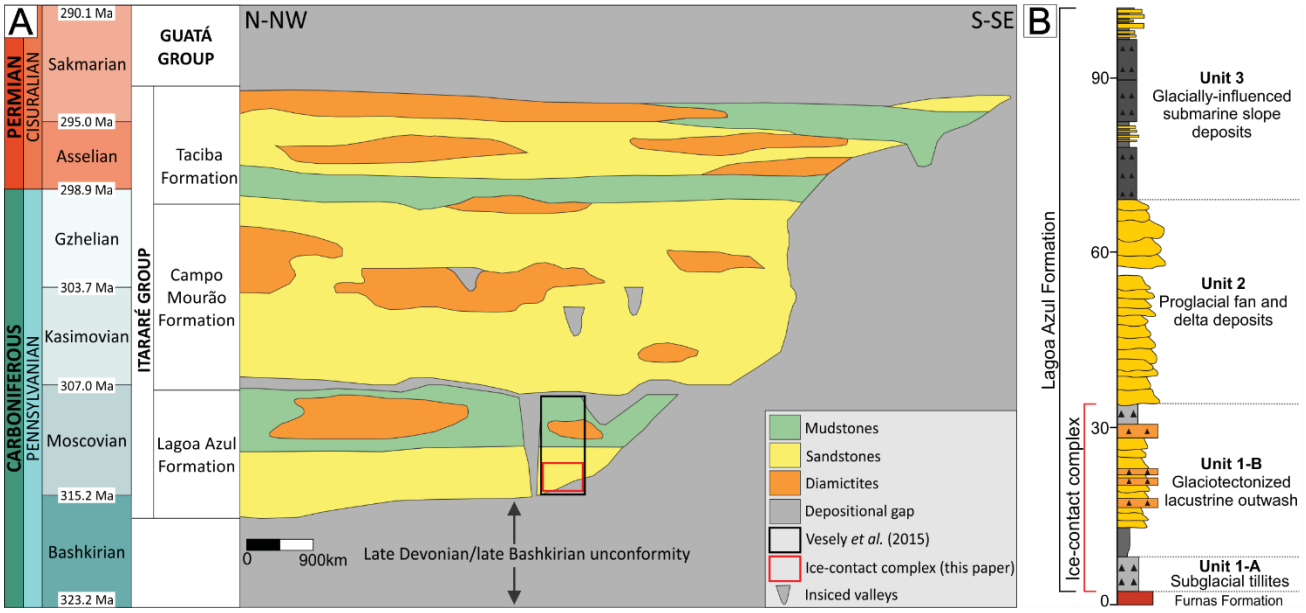

Figure 1 – **(A)** Stratigraphic chart of the Itararé Group in the eastern border of the Paraná Basin with reference to the stratigraphic position of the study interval (after França *et al.* 1996 and Holz *et al.* 2010; ages updated from Cohen *et al.* 2013). **(B)** Composite stratigraphic section adapted from Vesely *et al.* (2015) of the Lagoa Azul Formation in southeastern Paraná state with their individualized informal units and its respective interpreted depositional environments. The ice-contact complex analyzed in this study comprises units 1-A and 1-B.

Since the bulk of the Itararé Group comprises marine and transitional sequences interpreted as major deglacial cycles (França and Potter 1988, Vesely and Assine 2006), most research are concerned in characterizing its stratigraphic record based on traditional basin analysis approach in which glacial extent and cyclicity can be only inferred indirectly from stacking patterns and key surfaces (e.g. Canuto 1993, Vesely and Assine 2004, d'Ávila 2009, Puigdomenech *et al.* 2014, Buso *et al.* 2017, Vesely *et al.* 2018). Only at a few isolated localities placed at the lowermost portion of Itararé Group are documented thin intervals accumulated in subglacial and ice-marginal (ice-contact) settings where a direct

glacial signature can be observed as an assemblage of erosional, depositional and deformational geological products (Tomazelli and Soliani 1997, Vesely *et al.* 2015).

Late Paleozoic glaciers kineto-indicators of the Paraná Basin are mainly erosional and documented just on the nonconformity that underlies the Itararé Group and show patterns of ice-flow towards N and NW (e.g. Rosa *et al.* 2016, Fallgatter and Paim 2017). However, in between the Itararé Group deposits such landforms are absent and the glaciers kinematics are inferred indirectly by paleocurrent obtained in glacially-influenced and proglacial deposits (Carvalho and Vesely 2016, Mottin *et al.* 2018) and by rare beds comprising glaciotectonic structures (Rocha-Campos *et al.* 2000, Aquino *et al.* 2016).

Among previously reported localities containing an ice-contact sedimentation, the one exposed in southeastern Paraná State (Balsa Nova region; Bigarella *et al.* 1967, Trosdtorf *et al*. 2005, Vesely *et al.* 2015) is remarkable because of a relatively thick (several tens of meters) succession containing a rich archive of glaciogenic deposits and features (Fig. 1B). Taking into account that a combined analysis of co-genetic sedimentary facies, erosional landforms and deformational structures of glacial origin is the best approach to determine glaciers dynamics, glaciologic properties and glacial cyclicity (Benn and Evans 2010), in this paper we examine in detail this lower Pennsylvanian ice-contact complex. Then, the main aims of this work encompass: i) definition of a detailed sedimentary framework with the depositional environments according to the sedimentation position in relation to the glacier zones; ii) description of glaciotectonic structures and assembly of deformation patterns; iii) determination of paleo-ice flow patterns and better resolution glacial cyclicity of ice-margin fluctuations; and iv) evaluation of paleoglaciologic properties and local paleogeographic significance of the ice-contact complex.

3.2 GEOLOGICAL SETTING

The studied succession is exposed at the present eastern margin of the Paraná Basin around the localities of Balsa Nova, São Luiz do Purunã and Witmarsum, SE Paraná state (Fig. 2). It is equivalent to the basal portion of the lower third of the Itararé Group (Lagoa Azul Formation) and embraces units “1-A” and “1-B” as individualized by Vesely *et al.* (2015) (Fig. 1). The succession rests by a mild angular unconformity on early Devonian sandstones of the Furnas Formation at central and northern portions of the area, differently from the southern portion where is placed over a nonconformity on Precambrian phyllites of the crystalline basement (Fig. 2). Is capped by glacially-influenced proglacial subaqueous fan and deltaic deposits defined as “unit 2” by Vesely *et al.* (2015). Strata dip 5-10° to the west-southwest due to post-Paleozoic tectonic tilting driven by uplifting of the Ponta Grossa Arch (Strugale *et al.* 2007).

The presence of glaciogenic features in this area has long been reported, including striated surfaces and tillites on the Devonian substrate (Fuck 1966, Muratori 1966, Bigarella *et al.* 1967, Trosdtorf *et al.* 2005, Canuto *et al.* 2010). Vesely *et al.* (2015) proposed that the study interval was deposited as an ice-contact complex controlled by an unconfined, fluctuating terrestrial ice margin that advanced towards the north and northwest during two glacial cycles of advance and retreat. These authors interpreted the associated facies as subglacial tillites (unit 1-A) and glaciotectonized lacustrine outwash (unit 1-B) (Fig. 1B). Although considered Pennsylvanian because of the regional framework, the exact age of these deposits is poorly known because of the absence of fossiliferous horizons and syndepositional volcanic layers. An age not younger than Moscovian (315 to 307 Ma) is indicated by palynomorphs found in glaciomarine rhythmites of unit 3 some meters above the ice-contact complex (Kipper 2014, Kipper *et al.* 2017).

Figure 2 – Geological map of the study area with the indication of main outcrop localities and ice-flow directions obtained from subglacial striated surfaces, glaciotectonic structures and paleocurrents discussed in the text.

3.3 METHODS

This research was conducted through field examination of sedimentary facies, exhumed erosive landforms and penecontemporaneous soft-sediment deformational structures in a total of 44 outcrops in the Balsa Nova region, SE Paraná state. The lithotype classification scheme of Hambrey and Glasser (2012) was employed to facies definition because of the abundance of poorly-sorted facies. Six vertical stratigraphic sections were measured in a 1:50 scale containing about 273 m of total strata. Among these, a main stratigraphic section about 85 m-thick comprising all units discussed in the text was generated at outcrops located in a railroad track (localities 2 to 10; Fig. 2) and used for a guideline in the analysis of vertical facies association changes and glacial cyclicity.

In order to characterize the deformational styles and kinematics of glaciotectonic structures, panoramas were acquired and interpreted along laterally continuous outcrops. Also, 1193 measurements of deformational structures interpreted as of glaciotectonic origin, such as mm- to m-sized shear planes/surfaces, folded bedding and slickensides were taken and analyzed in pole-to-plane equal-area stereographic projection. Paleo-ice flow was inferred from the up-glacier dip direction of glaciotectonic features (e.g. Miller 1996, van der Wateren 2002, Phillips 2018). Seven subglacial striated/grooved surfaces on bedrock and intraformational surfaces were measured, five of them reported for the first time in the present paper. In addition, 705 paleocurrent data were taken from current- and climbing-rippled sandstones and cross-stratified sandstones and conglomerates and analyzed in synoptic rose diagrams to each individualized interval.

3.4 STRATIGRAPHIC FRAMEWORK

The combined analysis of sedimentary facies (Table 1), stacking patterns, deformational styles and the orientation of glacier kineto-indicators and paleocurrents allowed the definition of four informal stratigraphic units (Fig. 3). These include unit 1-A as previously defined by Vesely *et al.* (2015) and three units equivalent to unit 1-B of the same authors, here termed 1-B lower, 1-B middle and 1-B upper (Figs. 1B and 3A). Such ice-complex units compose an up to 80 m-thick vertical profile that shows a higher vertical expression than the 35 m-thick previously proposed.

Table 1 – Described sedimentary facies with respect of its depositional and deformational aspects.

F	Lithology	Depositional and deformational structures	Formative processes
F1	Sandy, clast-poor diamictite comprising faceted and bullet-shaped clasts ranging from granule- to cobble-size dispersed in a homogeneous matrix	Massive with subhorizontal cm-spaced anastomosing shear planes. Floored by striated pavements and topped by intraformational soft-sediment surfaces containing grooves, flutes and ridges	Debris accumulation and homogenisation by simple shear below an advancing glacier on bedrock
F2	Homogeneous, muddy to intermediate, clast-poor diamictite with striated, bullet-shaped and faceted clasts ranging from granule to cobble	Massive and showing subhorizontal mm- to cm-spaced shear planes. Clasts are oriented parallel to shear trend. Locally displays slickensides at the contact with other facies	Simple shear deformation and homogenisation imposed by an advancing glacier over non-consolidated sediments
F3	Polymictic, sandy, clast-rich diamictite with rounded to faceted clasts up to boulders	Arranged in tabular strata up to 2 m-thick; internally massive with incipient long-axis clast orientation. Sometimes floored by concave-up surfaces. Commonly grades to massive and current-rippled sandstones	Deposition from concentrated to hyperconcentrated meltwater flows emanated from tunnels at the glacier margin. Indicative of high meltwater discharge
F4	Sandy to intermediate, clast-poor diamictite with heterogeneous to homogeneous matrix and clasts ranging from granules to pebbles	Tabular beds up to 1 m-thick with relicts of current-ripples displaced by several small normal faults. Grades upwards to current-rippled sandstones	Resedimentation by slumps in a subaqueous setting
F5	Intermediate, clast-rich diamictite with granule to cobble-sized clasts	Internal faint stratification defined by mud/fine-sand laminae	Association between iceberg rain-out and settling of hypopycnal plumes
F6	Polymictic conglomerate with clasts up to boulders in a sandy matrix	Massive to faint-stratified, with a irregular basal contact containing flame structures. Metric intermediate diamictite (F5) rip-up clasts at the base	Deposition from subaqueous hyperconcentrated and highly erosive flows close to the glacier margin. Indicative of water-saturated sediments and rapid sedimentation
F7	Oligomictic conglomerate with sandy matrix	Mid-scale planar and trough cross stratification. Foresets often grade downflow to gravelly sandstones	Dune migration under high-energy bedload-dominated flows
F8	Medium-grained to gravelly sandstone. Clasts up to boulders occur dispersed	Tabular and concave-up strata with low- to medium-angle planar and trough cross stratification	Dune migration under high-energy bedload-dominated flows combined with deposition from iceberg rain-out
F9	Well-sorted muddy to medium-grained sandstone containing outsized clasts up to cobbles	Sinuous crested current ripples	Migration of subaqueous ripples under lower flow regime conditions and coeval iceberg rain-out
F10	Well-sorted, fine-grained sandstone. Locally display rare outsized clasts up to pebble-size	Sets up to 5 cm comprising climbing ripples with mud drapes on the foresets	Deposition from turbidity flows plus iceberg rain-out and hypopycnal plume settling
F11	Fine- to coarse-grained sandstones	Massive; often grades upwards to current-rippled sandstones	Slumps with concentrated density flow character triggered by gravity in a subaqueous setting
F12	Heterolithic facies defined by an alternation of fine-grained sandstone and mudstone laminae.	Rhythmic laminae (mm- to cm-thick) displaying normal grading between mud/sand pairs. Laminae sets are fairly truncated. Locally, sandy laminae occasionally have small current ripples and muddy laminae are thicker. Granule-sized clasts pierce the lamination.	Deposition from a combination of turbidity flows, iceberg rain-out and settling of hypopycnal plumes
F13	Mudstones and sandy mudstones with dispersed clasts up to cobbles	Massive	Fast mud settling from hypopycnal plumes associated with minor iceberg rain-out
F14	Muddy fine-grained sandstone with rare, up to cobble size, bullet-shaped and faceted clasts	Massive and heterogeneous matrix with remnants of current and climbing ripples and horizontal lamination. Pervasive subhorizontal mm- to cm-spaced shear planes. Stretched out mudstone clasts. Outsized clasts deform the remnants of stratification	Glaciotectonic deformation of subaqueous facies (F9, F10, F12, F13) imposed by subglacial and ice-marginal shear during a glacier advance

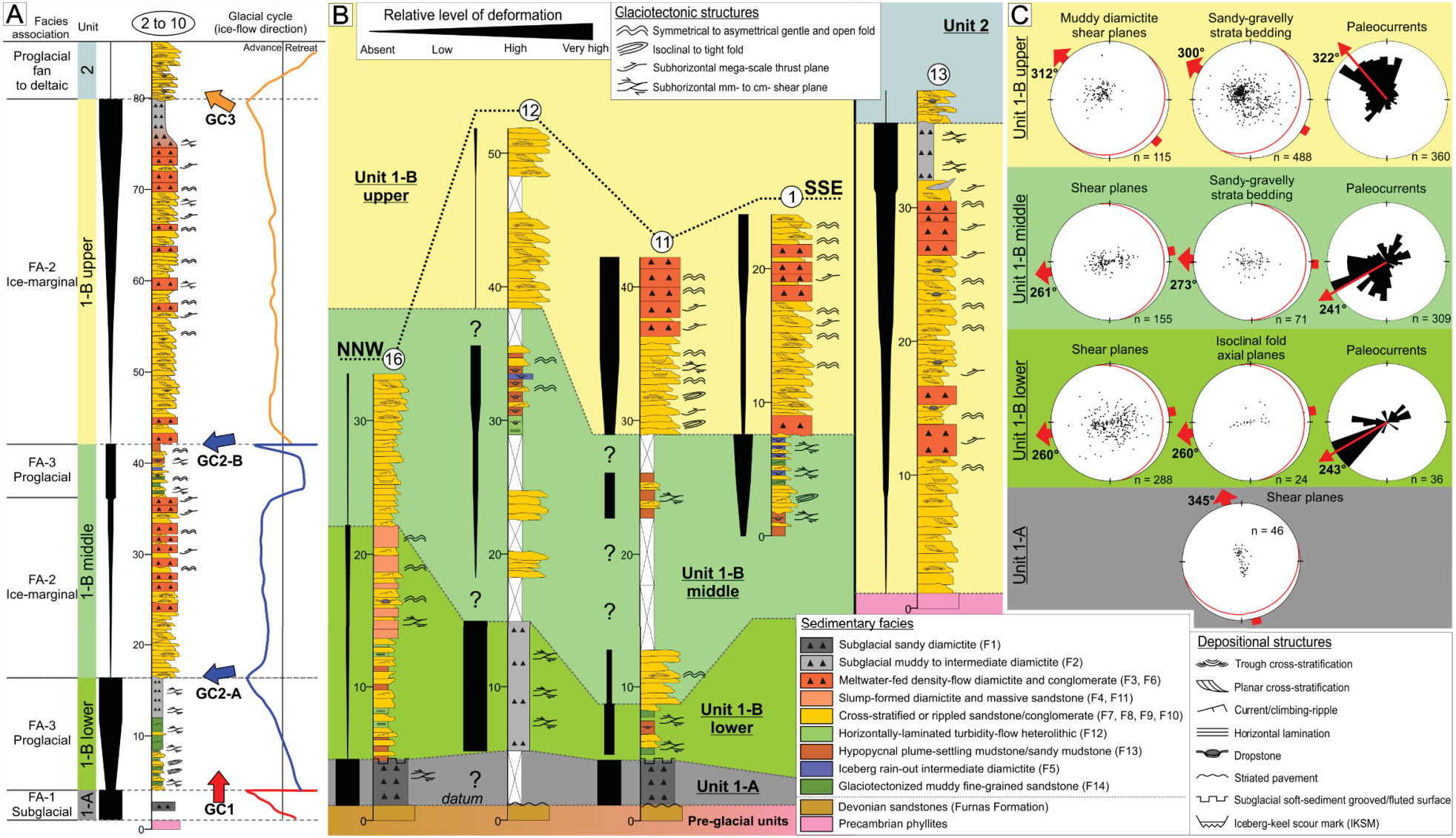

Figure 3 – **(A)** Composite stratigraphic section measured in outcrops at railroad track (localities 2 to 10) showing individualized units, unconformities (gray dashed lines), relative level of deformation, facies associations, glacial cycles and interpreted ice-flow directions. **(B)** Measured stratigraphic sections with a NNW-SSE correlation of sections located in figure 2 and architectural framework of the defined units showing high facies lateral change and thickness variation. Inferred deformational rates bars appears next to each section. Datum for correlation is the flat basal unconformity. **(C)** Pole-to-plane stereographic projections of soft-sediment deformational structures and synoptic rose diagrams with paleocurrents discussed in the text referent to each individualized unit.

The component facies and their interpreted depositional/deformational formative processes are shown in table 1. Most facies are, at some extent, modified by subsequent deformation whose intensity varies vertically throughout the stratigraphic succession. All stratigraphic boundaries are marked by unconformities and abrupt changes in the deformation rates (Fig. 3A-B).

The following subsections present a brief description of the outcrop expression of each defined unit and their component sedimentary facies, stacking patterns and soft-sediment deformational structures. Kineto-indicators are presented to each unit by stereographic projections of soft-sediment deformational glaciogenic structures and synoptic rose diagrams with paleocurrent measurements (Fig. 3C).

3.4.1 Unit 1-A and basal unconformity

The unconformity that underlies the studied succession is defined by a flat surface containing five striated pavements carved on Devonian sandstones. No striated surfaces were found over Precambrian metamorphic rocks. These pavements over Furnas Formation have an area of up to 2500 m², comprise straight and parallel shallow grooves, ridges and striation with a north-south mean orientation with a minor variation related to its spatial distribution. At Witmarsum locality, at northwesternmost portion of the study area, the grooves and striation over the surface documented by Bigarella et al. (1967) (locality 18) show a 358° orientation and over a, herein first-time reported striated, pavement at locality 19 a 355° orientation (Fig. 4A). On other hand, three first-time reported pavements placed along the margins of Mortes River at the eastern region (localities 11, 12 and 14) comprise shallow grooves and striation oriented toward 6° to 10° azimuth (Fig. 4B-D). At one of these surfaces (locality 12; Thalia Club), several crescentic gouges up to 15 cm-large indicate a northward sense of ice-flow (Fig. 4C).

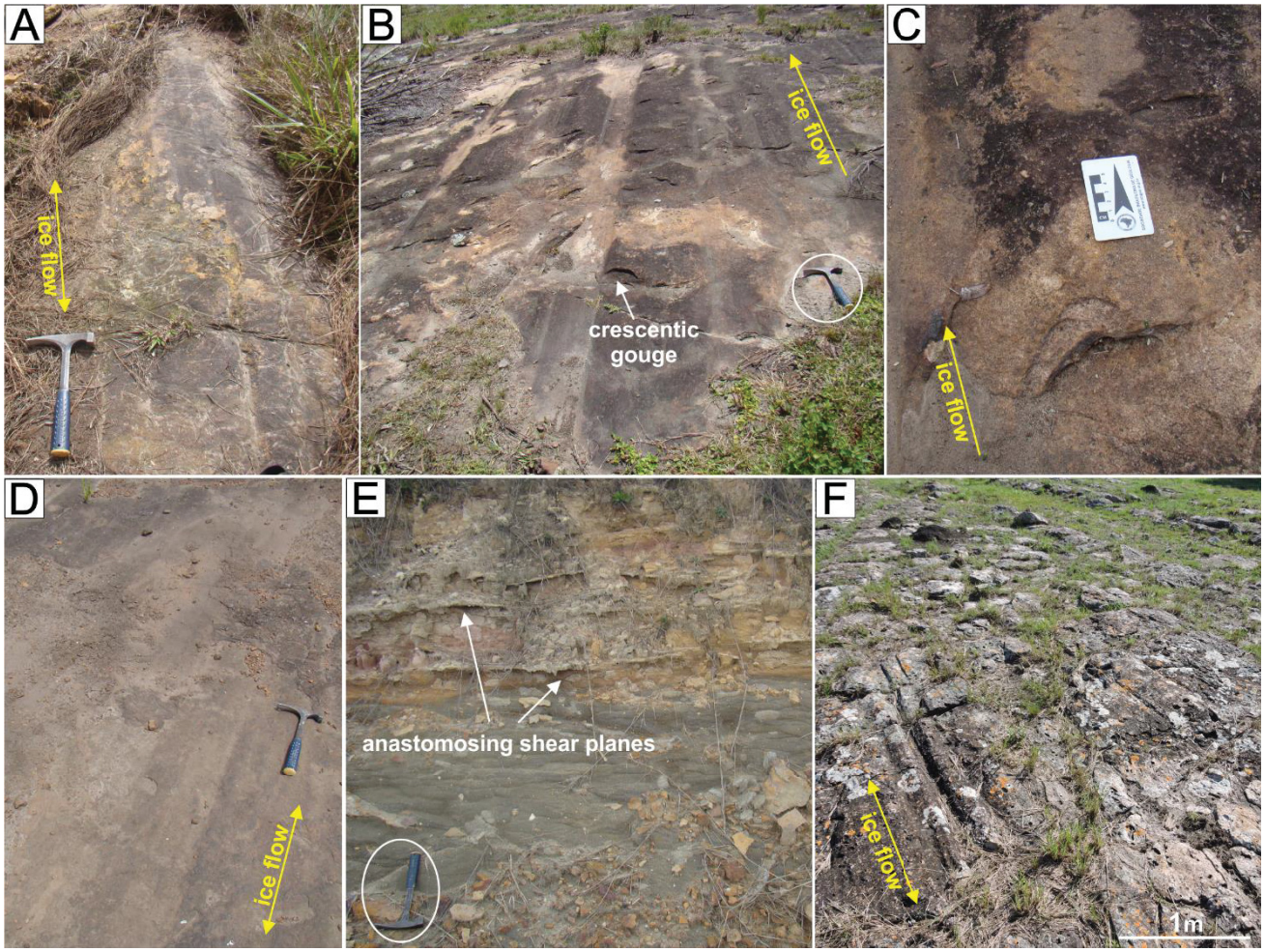

Figure 4 - Main facies and erosive features related to unit 1-A: **(A)** Striated surface on Devonian Furnas sandstones at Witmarsum (locality 19). **(B)** Flat grooved/striated surface on Devonian Furnas sandstones at Thalia Club (locality 12). Ice flow is toward the upper part of the picture evidenced by crescentic gouges. **(C)** Detail of a concave up-glacier crescentic gouge over the Thalia Club striated surface (locality 12). **(D)** Shallow striation over Furnas sandstones near Mortes River (locality 11). **(E)** Massive clast-rich sandy diamictite (F1) with subhorizontal anastomosing shear surfaces highlighted by oxide infiltration at the upper portion. **(F)** Flat soft-sediment subglacial surface near Mortes River (locality 11) developed on top of diamictites containing grooves and ridges oriented to NNE-SSW (8°-188°) similarly to striation/grooves on Furnas sandstones. No clear kinematic indicators are found on this surface.

Resting above this unconformity, sandy, clast-rich, massive diamictites up to 7 m-thick (F1) occur discontinuously through the area. The diamictites are non-stratified, but their matrix shows cm-thick, non-continuous, anastomosing subhorizontal shear planes (Fig. 4E) that show a mean dip direction towards SSE (N165/10) and a stress vergence/ice-flow direction towards NNW (mean azimuth = 345°; Fig. 3C). Clasts are mainly sub-rounded and secondarily faceted to bullet-shaped, can reach up to cobble-size, but pebbles predominate. Furthermore, the upper boundary of the diamictites is characterized by a laterally extensive flat surface comprising grooves, ridges and flutes. In addition to the

surface previously documented by Trosdtorf *et al.* (2005) at locality 15 where asymmetric small flutes indicate a northward ice-flow direction (mean azimuth = 2°), another surface placed at locality 11 comprises parallel deep grooves and ridges oriented in a NNE-SSW direction (8°-188° azimuth) with no clear indicator of ice-flow direction, however clearly correlated to the surface at locality 15 (Fig. 4F).

3.4.2 Unit 1-B lower

This unit is up to 18 m-thick and is variable in terms of composition and deformational patterns (Fig. 3). In a depositional pre-deformational context, it consists of an association of fine-grained facies that includes an intercalation of current-rippled fine- to medium-grained sandstones (F9; Fig. 5A), climbing-rippled fine-grained sandstones with mud drapes on foresets associated with laminated heterolithics (F10, F12; Figs. 5B-C) and massive sandy mudstones with dispersed outsized clasts (F13). Locally, sandy to intermediate clast-poor diamictites with relicts of current-ripples displaced by cm-sized normal faults (F4) occur at the top of the succession intercalated with massive (F11) and current-rippled fine-grained sandstones beds (Fig. 5D-E).

Such unit is characterized by rare outsized clasts dispersed in strata and by a coarsening-upward pattern that exhibits mainly mudstones, fine-grained sandstones and heterolithics at the base grading to medium-grained massive and current-rippled sandstones and sandy to intermediate clast-poor diamictites towards the top (e.g. section 16; Fig. 3B). At the whole unit paleocurrents from non-deformed current-rippled sandstones show a southwestward trend (243° mean azimuth; Fig. 3C).

Different deformational patterns take place at different localities where facies are non- to highly-deformed. At locality 2, a railroad cut shows a 10 m-high succession with a distinct upward variation in deformation patterns and homogenisation rates (Figs. 6A-H). The original beds of fine- to medium-grained, rippled sandstones and heterolithics

predominate in the lower portion of the exposure and are disposed in rootless isoclinal folds with subhorizontal axial planes (Fig. 6B) verging westward (80/10 mean dip direction; Fig. 3C). In the middle portion these sandy layers become more boudinaged and disrupted (Fig. 6G) and in the upper portion are absent.

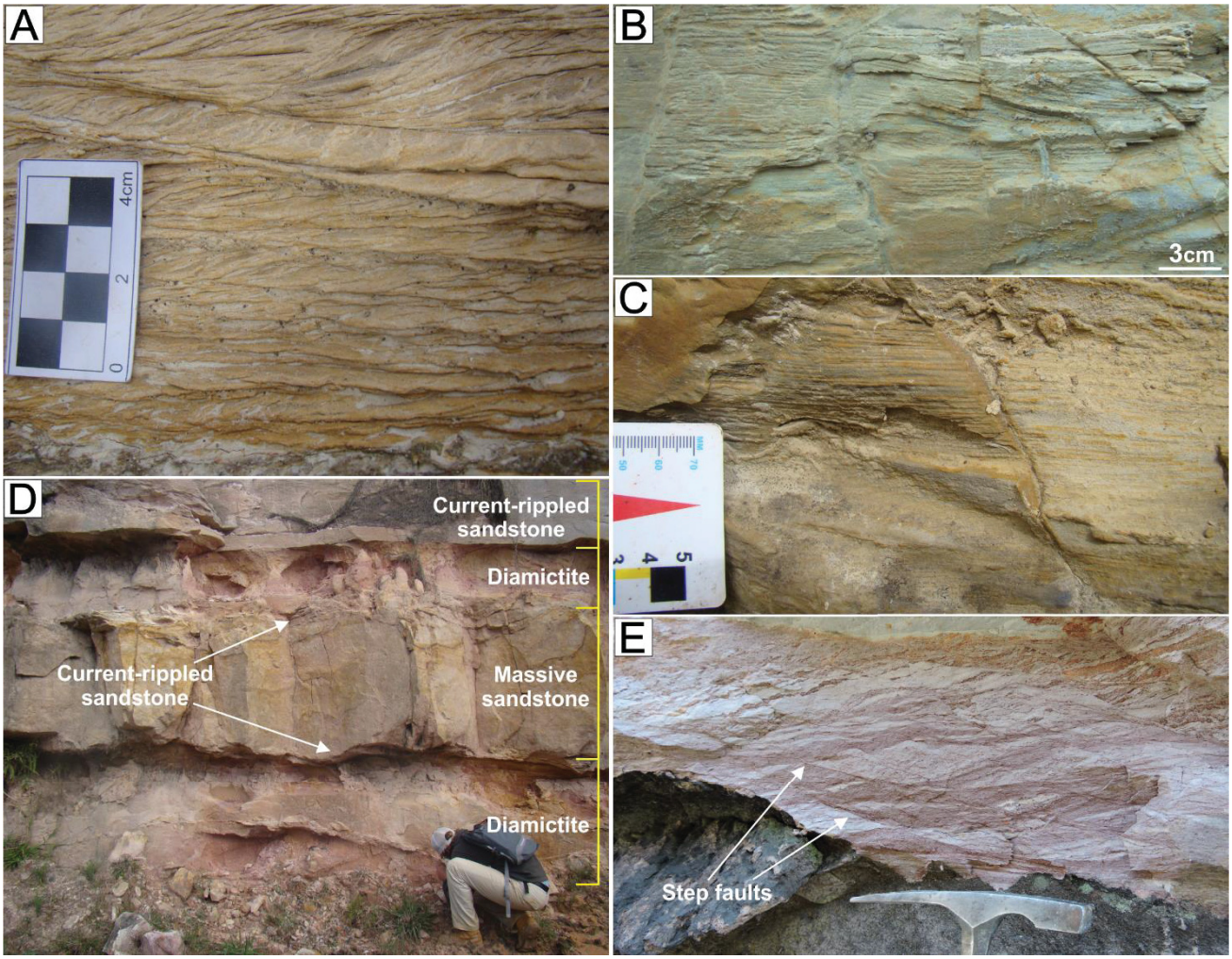

Figure 5 – Sedimentary facies of lower portion of unit 1-B: **(A)** Current-rippled fine-grained sandstones (F9). **(B)** Climbing-rippled fine-grained sandstones with mud drapes on foresets (F10) associated with laminated heterolithics (F12). **(C)** Laminate heterolithics with mm-thick fine-grained sand/mud pair (F12). **(D)** Gently deformed intercalation between fine-grained (F9) and massive sandstones (F11) with clast-poor sandy to intermediate diamictites with **(E)** relicts of current ripples dislocated by small normal faults (F4).

Muddy fine-grained sandstones with a massive and heterogeneous matrix containing relicts of ripples and horizontal lamination as well stretched mud clasts and outsized clasts (F14; Figs. 6C-E) appear in the lower portion between the sandy layers and at the middle portion consist in the predominant facies. On other hand, the upper portion of the exposure is characterized by massive homogeneous intermediate clast-poor diamictites (F2; Fig. 6F).

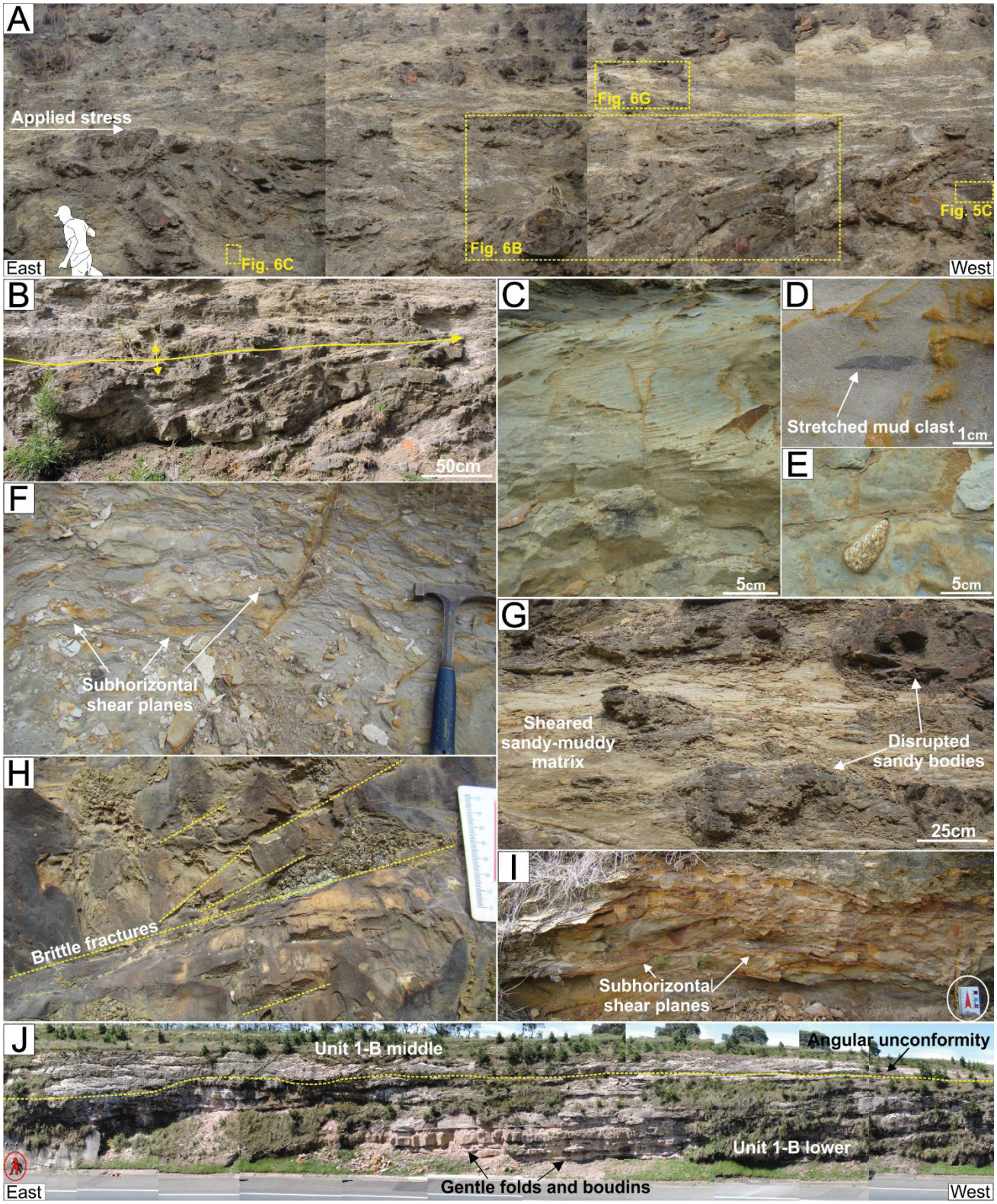

Figure 6 – Main deformational structures and patterns of unit 1-B: **(A)** Lower and middle interval of railroad cut (locality 2) with deformed strata disposed in **(B)** isoclinal folds at the base and more homogenised toward the top. **(C-E)** Muddy fine-grained sandstones containing relicts of depositional structures, stretched mud clasts and dispersed outsized exotic clasts (F14). **(F)** Sheared intermediate diamictite (F2) disposed at the top of the railroad cut. **(G)** Detail of the middle portion of the exposure with high density of subhorizontal shearing and disrupted sandstone bodies. **(H)** Detail of sandstone bodies with relicts of current-ripples with brittle joints. **(I)** Intermediate clast-poor diamictite with subhorizontal anastomosing cm-spaced shear surfaces at locality 12. **(J)** Gently folded and boudinaged top layers of unit 1-B lower at locality 16 under a low-angle angular unconformity (yellow dashed line) overlaid by undeformed sandstones of unit 1-B middle.

Mm- to cm-spaced subhorizontal anastomosing shear planes highlighted by oxides occur in the whole succession but are more abundant in the middle and upper portions of the exposure in the matrix of muddy fine-grained massive sandstones (F14; Fig. 6G) and intermediate diamictites (F2; Fig. 6F). In the sandy bodies at the bottom, the original depositional structures are often dislocated by several brittle fractures dipping to east (Fig. 6H).

Locality 12 exhibits an 8 m-high exposure of muddy to intermediate, clast-poor diamictite with a homogeneous matrix and no preserved depositional structures (F2). The diamictite is cut by several subhorizontal, anastomosing, cm-spaced shear surfaces highlighted by oxide infiltration (Fig. 6I). Some disrupted bodies of sandstone occur dispersed throughout the exposure. The sandy-muddy character of the diamictite matrix, the similarity of the deformational structures and its stratigraphic position allow placing this outcrop in the same level than the upper portion of locality 2 where the sheared diamictite sits on folded heterogeneous strata. Measured low-angle, shear surfaces in all outcrops of unit 1-B lower are undulated and show a moderate degree of dispersion (Fig. 3C). Despite that, the stereographically calculated mean vector (288 measurements) resulted in a dip towards ENE (N80/10) and an applied stress vergence to SSW (260°).

At locality 16 the facies intercalation that configures the upper portion of unit 1-B lower is very well preserved, displaying slightly to non-deformed tabular strata of an alternation of beds of massive and fine-grained current-rippled sandstones and intermediate clast-poor diamictites with a high abundancy of step faults dislocating current-ripples (F4). Strata are tilted in low angles to the east, exhibit gentle symmetrical folds and some reverse faults with an eastward kinematics as well some layers are slightly boudinaged (Fig. 6J).

3.4.3 Unit 1-B middle

These deposits are up to 25 m-thick and rest on the previous unit by means of an angular unconformity (Fig. 6J). It comprises two facies associations bounded by a distinct sharp contact (Figs. 3A and 7A). The basal association is an up to 20 m-thick, sandy-gravelly, coarsening-upward interval composed of amalgamated, tabular beds of well- to poorly-sorted cross-stratified sandstones and conglomerates (F7, F8, F9; Fig. 7A) and sandy, clast-rich, massive diamictites (F3; Fig. 7B). This association is not regularly distributed through the study area and may be absent or with reduced thickness in some localities. Laterally discontinuous, soft-sediment grooved and striated surfaces with internally small sand slumps are present on top of sandstone bedding planes (Fig. 7C).

The upper association is an about 7 m-thick fine-grained succession mainly composed of intercalated beds up to 60 cm-thick of fine- to medium-grained current-rippled sandstones (F9) and muddy fine-grained heterogeneous sandstones with relicts of current-ripples (F14; Fig. 7D). Outsized clasts of lithified sandstones (Fig. 7E) and igneous/metamorphic origin occur throughout the fine-grained beds. Laminated heterolithics with cm-thick sand/mud pairs (F12) occur mainly associated with massive mudstones to sandy mudstones with outsized clasts (F13) and intermediate massive to faint-stratified clast-rich diamictites (F5) (Fig. 7F-I). Paleocurrents from both facies associations that form unit 1-B middle display an asymmetric bimodal pattern with a main mean vector to SW (241°) and a subordinate one to NE (Fig. 3C).

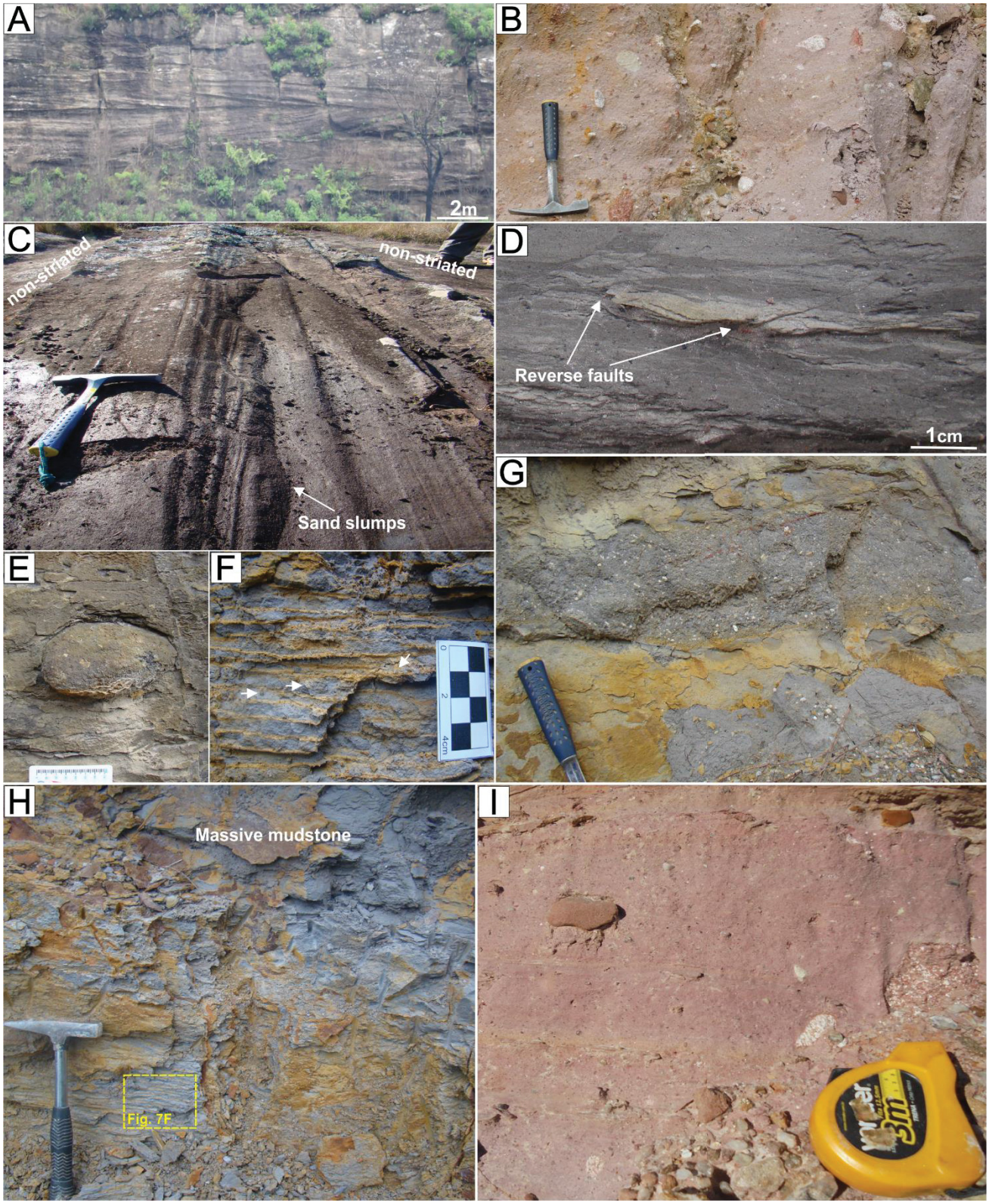

Figure 7 - Main sedimentary facies of unit 1-B middle: **(A)** Large-scale cross-stratified sandstones and conglomerates (F7, F8). **(B)** Massive, sandy, clast-rich diamictites (F3) that predominate at the top of sandy-gravelly association. **(C)** Soft-sediment striated surface developed on top of sandstone beds with a cross-cutting pattern with small striated slumped sand directed into a major trough. **(D)** Partially deformed muddy fine-grained current-rippled sandstones (F14) with remnants of ripples dislocated by small reverse faults. **(E)** Outsized lithified sandstone clast immersed in muddy fine-grained sandstones (F14). **(F)** Heterolithics with cm-thick sand/mud pair (F12). White arrows indicate pebbles. **(G)** Intermediate clast-rich diamictite layer (F5) grading from massive mudstones (F13). **(H)** Laminated heterolithics below grading upwards to massive mudstones with dispersed clasts (F13). **(I)** Faint-stratified clast-rich diamictite (F5).

This unit exhibits an upward increase in deformation rates (Fig. 3) from an undeformed basal portion of the sandy-gravelly association to a highly sheared and folded upper fine-grained association at the top (Fig. 8). At locality 4 (Eng. Bley station), the upper portion of the sandy-gravelly association and the base of the fine-grained association display gentle to open, symmetric to somewhat asymmetric, synclines and anticlines that are truncated by mega-scale subhorizontal shear surfaces (Fig. 8A-B). Such folds are parasitic folds of a mega-scale gentle anticline. Fold axis are oriented N-S and a deformation vergence to W is stereographically calculated (273° mean azimuth; Fig. 3C) and observed in outcrop panoramas (Fig. 8A).

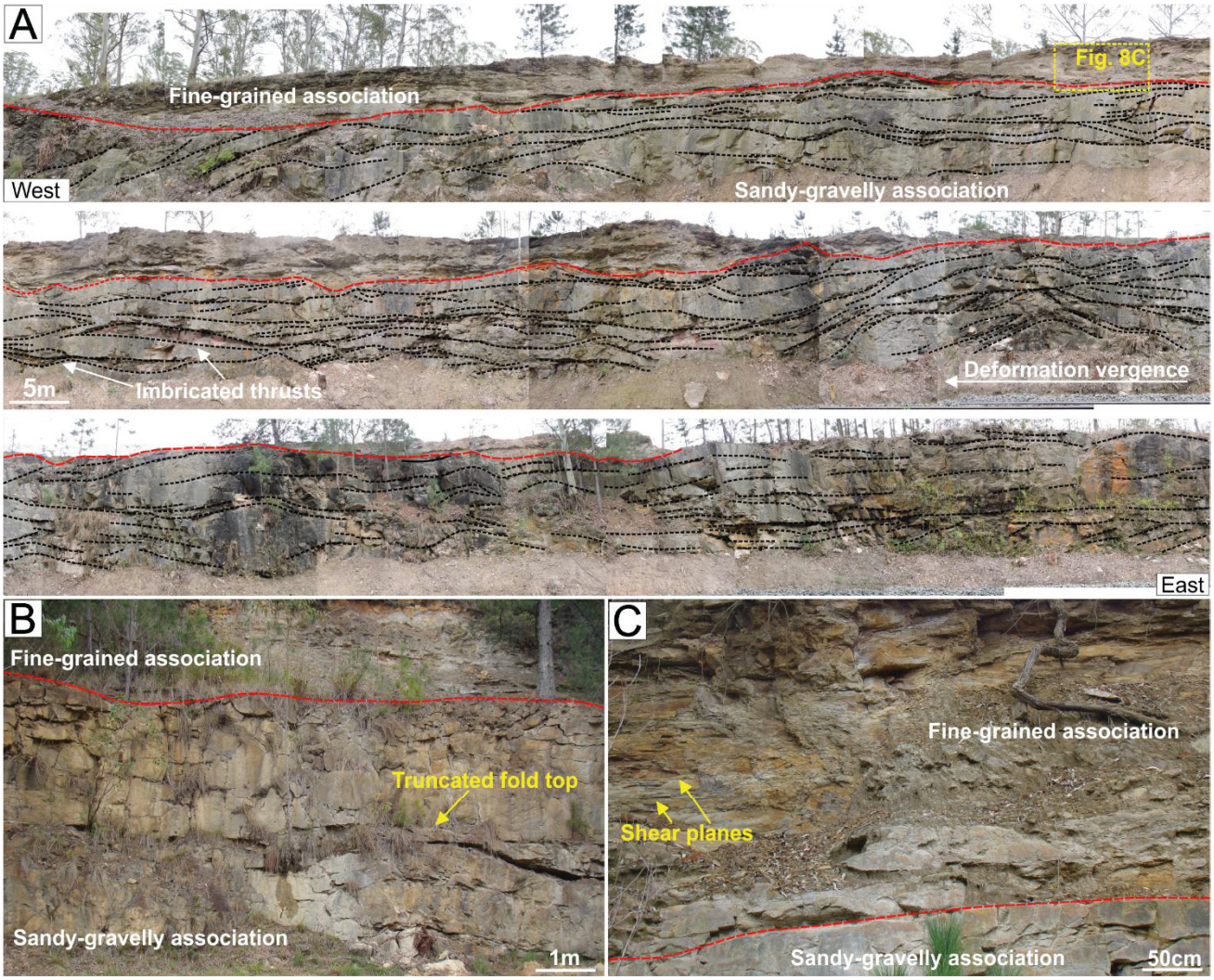

Figure 8 – Deformational patterns at unit 1-B middle at a railroad cut at Eng. Bley station (locality 4): **(A)** 300 m-long West-East panorama of the eastern limb of a mega-scale gentle anticline. The dashed red line represents a mega-scale shear surface that separates the gently- to open-folded sandy-gravelly strata (black lines) with low-angle imbricated thrusts below and the sheared fine-grained association above. **(B)** Detail of a truncation surface in between the sandy-gravelly association cutting the top surface of an open fold. **(C)** Detail of the basal portion of fine-grained association composed by heterogeneous highly-sheared muddy fine-grained sandstones (F11).

The whole fine-grained association presents subhorizontal centimeter shear surfaces and, at its sharp basal contact over the sandy-gravelly strata, high-density of cm-spaced shear surfaces in partially homogenised muddy fine-grained sandstone facies take place (Fig. 8C). Towards the top, the fine-grained association exhibits boudinaged muddy to fine-grained sandstone layers. Such layers and current-ripples are more well preserved in fine-grained sandstones, on other hand, sandstones with higher mud content present relicts of current ripples cut by mm- to cm-scale faults (Figs. 7D). The cm-spaced shear surfaces measured from the fine-grained association (Fig. 3C) resulted in a mean vector dipping in low angles to the ESE (N81/10), which indicate a westward applied stress field similar to the folded sandy-gravelly strata placed below.

3.4.4 Unit 1-B upper

The upper interval of unit 1-B is an up to 40 m-thick, erosive-based, sandy-gravelly succession. The basal boundary is uneven, at some places are over the metamorphic basement (e.g. section 13 in Fig. 3B). It comprises tabular beds of cross-stratified, well- to-poorly sorted sandstones and conglomerates (F7, F8, F9; Fig. 9A) with paleocurrents to the NW (322° mean azimuth; Fig. 3C) associated with massive, sandy, clast-rich diamictites, sandstones and conglomerates with metric mudstone rip-up clasts (F3, F6, F11; Fig. 9B-D). Facies change are observed in outcrop scale both vertically and laterally. Massive metric tabular beds of sandy diamictites usually grades upwards to dm-sized beds of massive medium-grained sandstones and to current-rippled fine-grained sandstones on top (Fig. 9D) whereas tabular beds of cross-stratified conglomerates rapidly grade downstream to gravelly sandstones (Fig. 9A).

Laterally discontinuous, containing marginal berms, soft-sediment striated surfaces are common over sandstone and conglomerate bedding planes. They in general reach dozens of m² in areal extension however can be up to 850 m² (Fig. 9E).

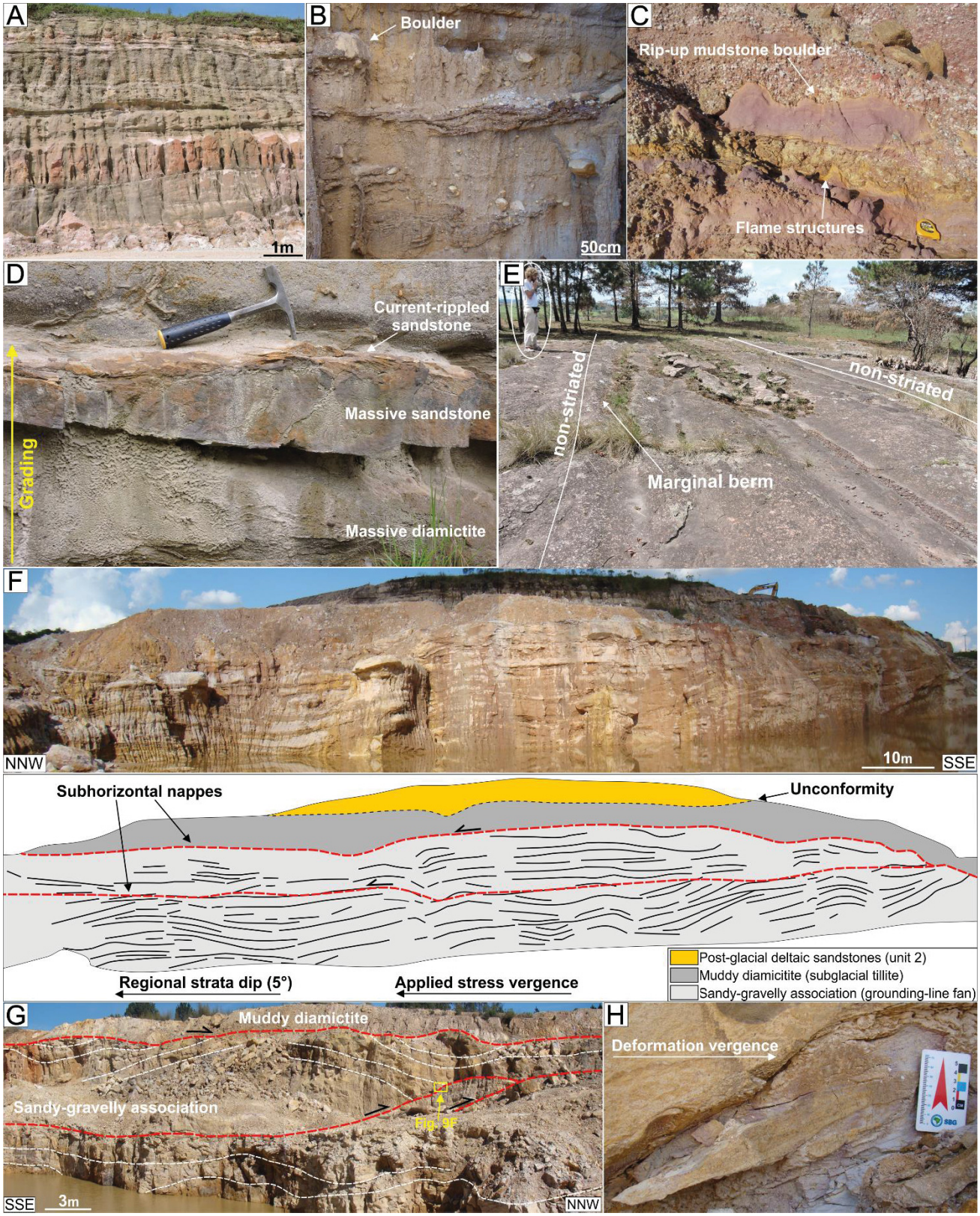

Figure 9 – Sedimentary facies and deformational patterns of unit 1-B upper: **(A)** Poorly-sorted, cross-stratified, amalgamated sandstones and conglomerates (F7, F8). **(B)** Deformed strata of massive, sandy, clast-rich diamictites with faceted clasts up to boulder-size (F3). **(C)** Flame structures at the contact between unit 1-B middle and 1-B upper with conglomerate with metric rip-up boulders of mudstone facies. **(D)** Bed with normal grading from massive sandy diamictites to current-rippled sandstones. **(E)** Laterally restricted soft-sediment grooved surface over non-deformed sandstones with shallow grooves inside an 85 m-long, 5 m-wide trough with a marginal berm in one of its extremities. **(F-G)** Exposures at Bassani sand pit (locality 13) with gently folded sandy-gravelly beds and muddy diamictite slabs juxtaposed by mega-scale subhorizontal shear surfaces represented by red dashed lines. **(H)** Detail of a shear zone with sigmoid sandstone lenses surrounded by a mud matrix.

This unit exhibits a heterogeneous deformational pattern both vertically and horizontally. In general, the base of the interval is not or slightly deformed and the soft-sediment deformation structures increase in frequency towards the top. However, at locality 11 the basal strata are highly deformed and somewhen disposed in close folds cut by medium- to low-angle cm-sized shear planes (Fig. 3B).

At locality 13, sandy-gravelly strata are affected by large open symmetrical to asymmetrical synclines and anticlines that are intercepted by mega-scale thrust surfaces (Fig. 9F-G). The thrusts are highly undulated, mainly disposed in a subhorizontal position but the dip can reach 50°. Internally, these thrusts define shear zones up to 40 cm-thick displaying cm- to dm-long sigmoidal sand bodies surrounded by a sheared fine-grained matrix (Fig. 9H).

At localities 6 to 10, which consist of up to 300-m-long railroad cuts, sandy-gravelly facies show a clear upward increase in deformation and a decrease in the degree of preservation of original stratification. Mega-scale slightly asymmetrical open folds associated with thrust surfaces with a northwestward kinematics (Fig. 10A-B) occur in sets of beds at the middle portion of the unit. Towards the top the layers become progressively more deformed with current-rippled, fine-grained sandstone beds up to 50 cm-thick disposed in meso-scale isoclinal folds inside the m-thick deformed sandy diamictite beds (Fig. 10C). Such common structures at this level are brittle-dominated small normal faults dipping to NW associated with boudinaged layers of fine-grained sandstones (Fig. 10D) and the dominance of subhorizontal to medium-angle cm-thick shear surfaces that defines de axial plane of isoclinal folds and are immersed in the sandy diamictites matrix (Fig. 10C). Randomly-disposed brittle fractures also occur in some portions (Fig. 10C).

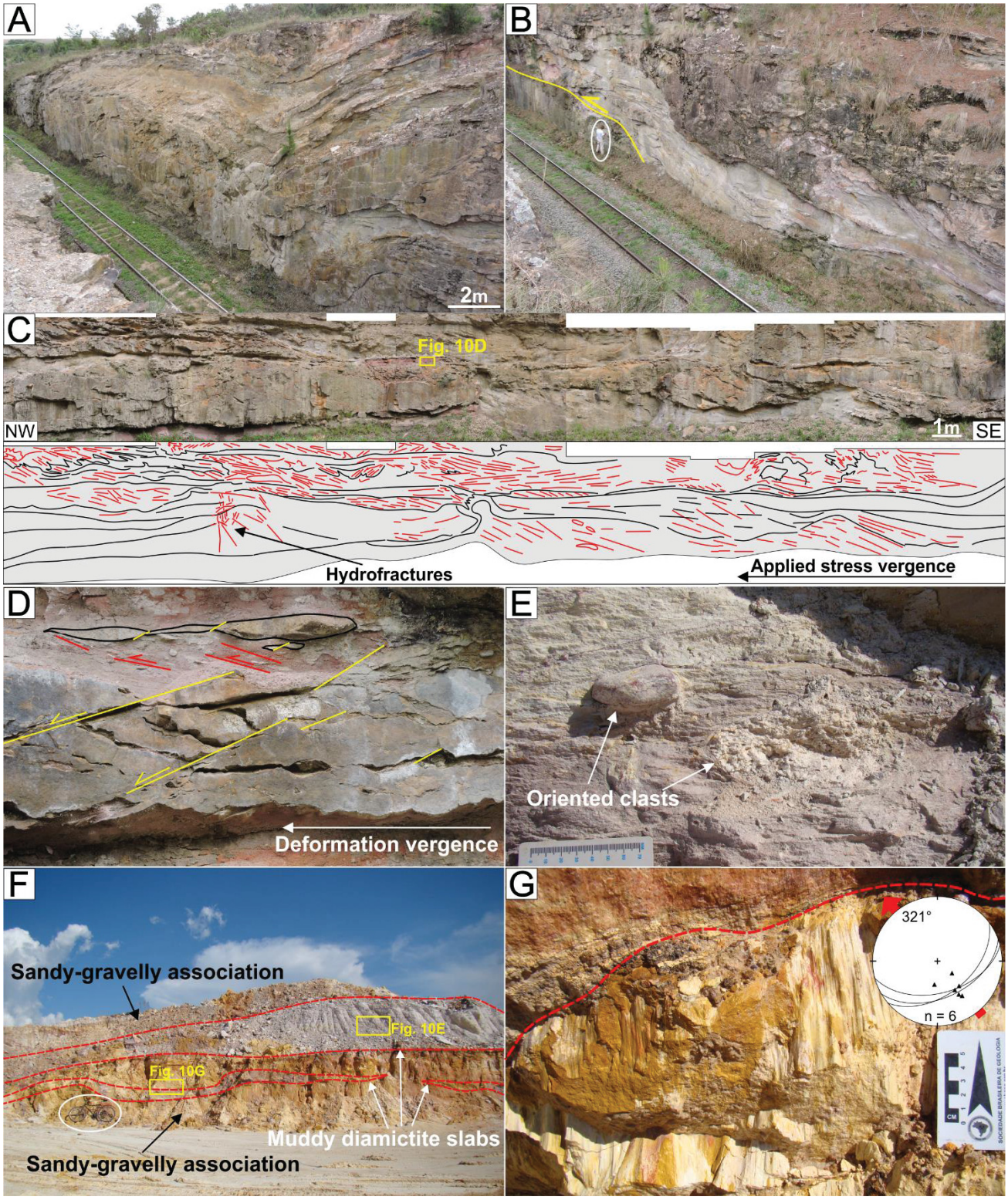

Figure 10 – Sedimentary facies and deformational patterns of unit 1-B upper: **(A)** Sandy-gravelly facies arranged in a large gently asymmetrical syncline with a truncated limb associated with **(B)** low-angle dipping thrust surface shown by a yellow line. **(C)** Sandy-gravelly association cropping out in a railroad cut at locality 9. Bedding remnants (black lines) of sandy-gravelly strata that are folded, boudinaged and cut by low- to moderate-angle cm-sized shear surfaces (red lines). **(D)** Small-scale normal faults (red lines) cutting fine-grained sandstone boudins and cm-long shear planes (yellow dashed lines) inside the sandy diamictite matrix. **(E)** Muddy, clast-poor diamictite with subhorizontal mm-thick shear surfaces and faceted clasts oriented parallel to shearing (F2). **(F)** Macro-scale muddy diamictite slabs between the top portions of sandy-gravelly association. **(G)** Slickensides at the contact (red line) between muddy diamictite and sandy-gravelly facies with stereographic projection showing a transport towards NW (321°).

A muddy to intermediate, clast-poor, massive diamictite facies with mm-spaced subhorizontal shear surfaces and clasts oriented parallel to shear trend (F2; Fig. 10E) takes place in the upper part of this unit. At locality 11 it occurs as lenticular, macro to mega-scale imbricated slabs up to 5 m-thick immersed in between sandy-gravelly strata (Figs. 9F-G and 10F) with abrupt subhorizontal sheared contacts often displaying slickensides (Fig. 10G). At locality 10 the same diamictite facies appears as a sheet-like body with a diffuse lower contact grading from underlying sandy-gravelly deformed facies (Fig. 3A).

Both sandy-gravelly facies and muddy diamictites of this unit exhibit deformational structures with a main deformation vergence towards NW (Fig. 3C). Millimeter-spaced shearing (Fig. 10E) inside muddy diamictites has a very consistent dip direction to SE (132/10 mean dip direction). This same deformation vergence is also indicated by fold asymmetry in the sandy-gravelly succession (mean azimuth = 300°) and by the dip towards SE of slickensides (mean azimuth transport = 321°; Fig. 10G).

3.5 DEPOSITIONAL SETTINGS

The examined succession intercalates slightly deformed/undeformed strata with highly deformed facies. In the deformed intervals deformation obliterated part or the totality of the original depositional structures, leaving in some cases only relicts that can be used to interpret sedimentary processes and depositional environments that operated prior to deformation. Observed sedimentary facies and stacking patterns allowed to insert these deposits in three facies associations related to the glacier zones that are recurrent throughout the stratigraphic succession: i) subglacial tillites (subglacial), ii) proximal grounding-line fan (ice-marginal), and iii) distal grounding-line fan (proglacial) (Fig. 11).

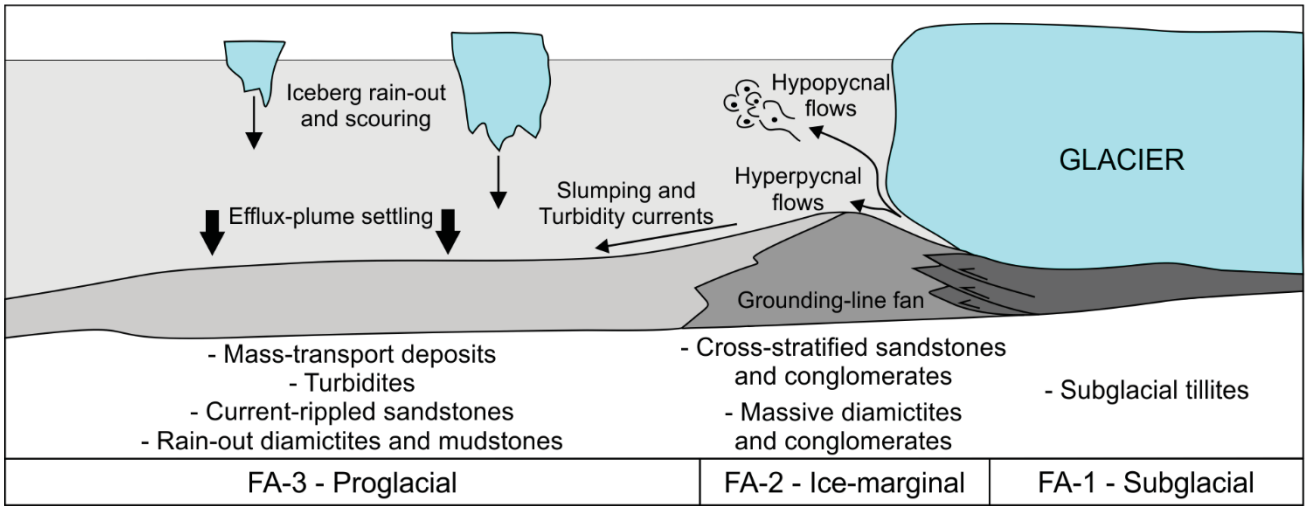

Figure 11 – Main depositional processes operating at different zones of a grounded warm-based glacier system and their respective sedimentary products (after Eyles *et al.* 1985, Ingólfsson 1987, Hart and Roberts 1994). Individualized facies associations are inserted in the subglacial, ice-marginal and proglacial zones.

3.5.1 Subglacial tillites

Sandy diamictites of unit 1-A (F1) were previously interpreted as a subglacial deforming layer (subglacial tillite) related to a single event of glacial advance over a pre-glacial substrate (Vesely *et al.* 2015). The presence of shearing, subglacial lineations both below and above these deposits and the absence of major internal discontinuities and/or interbeds corroborates this interpretation. In addition, some further considerations about subglacial processes can be offered by taking into account the compositional and structural properties observed in these diamictites.

As postulated by Evans *et al.* (2006), sandy tillites are porous and this porosity allows the deforming layer to be water-saturated, promotes strong ice coupling and consequent high rates of stress transmission from the ice to its basal layer. Therefore, the massive/homogeneous character of the diamictites and the subhorizontal anastomosing shear planes suggest a glacier coupled to its bed that moved mostly by subglacial sediment deformation (van der Meer *et al.* 2003). The sandy matrix character is interpreted as result of abrasion of Devonian Furnas sandstones that compose the paleo-bedrock.

The definition and individualization between processes operating at the subglacial zone is a difficult task since the constant glacier advance continue to transmit stress to its basal deforming layer. It results in a deformation superimposition what obliterate previous characteristics of another processes (i.e. melt-out, lodgement, sliding, subglacial meltwater flows) and give rise to texturally homogeneous diamictites as an end member, therefore termed subglacial traction till (Evans *et al.* 2006). The observed diamictites possess this homogeneous character that can be just interpreted as product of subglacial deformation. However, near the Witmarsum locality, at an exposure no more available, Canuto *et al.* (2010) identified a 10 cm-thick sheared diamictite layer placed just above a striated pavement over Furnas sandstones containing faceted clasts of Furnas sandstones embedded in a sheared sandy matrix. Their interpretation assumed an original tillite emplacement by lodgement in the glacier/bedrock interface after deformed by continuous glacier advance.

The top surfaces containing flutes, grooves and ridges were generated at the ice/sediment interface due to plowing when sediment strength was exceeded and the ice began to slide over the bed (Benn and Evans 2010). The subglacially abraded/plucked bedrock and the up to 7 m-thick deforming layer are evidence for a predominant wet-based basal thermal regime and relatively fast glacier flow by combination of soft bed deformation and bedrock abrasion (Boulton 1996, Bennett and Glasser 2009).

Such subglacial tillites differs in thickness and texturally from other occurrences placed on the Itararé Group basal nonconformity documented at other regions of Paraná Basin. Tillites settled on gouges, troughs and streamlined bedforms generated by glacial erosion on metamorphic and igneous rocks and interpreted as lodgement tillites (e.g. Almeida 1948, Tomazelli and Soliani 1997, Fallgatter and Paim 2017, Assine *et al.* 2018) are discontinuous and thin, being up to 80 cm-thick and comprise a higher amount of faceted local-sourced clasts than the herein analyzed diamictites.

The areal distribution of subglacial striated surfaces both on Devonian sandstones and over the subglacial tillite, as well as the shear planes orientation (Fig. 3C), ranging from a NNW to a NNE orientation (Fig. 2) is suggestive of a radial flow pattern and related to a glacier with a lobate termini, similar as Pleistocene ice lobe margins (e.g. Colgan and Mickelson 1997, Glasser *et al.* 2008). The emplacement of thick till sheets depends firstly on its location within the subglacial zone and is facilitated in subglacial environments that are relatively close to the ice margin since sediment produced at inner zones are transported by a combination of subglacial meltwater streams and glacier advance and accumulated towards the outer zone (Boulton and Deynoux 1981, Boulton 1996). According to that and taking into account the evidence for ice/sediment coupling and the radial pattern of subglacial striated surfaces, it is suggested that subglacial traction tillites of unit 1-A were emplaced in the subglacial outer zone, thus representing the marginal portions of an ice lobe.

The muddy to intermediate, clast-poor diamictites at the top of unit 1-B lower and 1-B upper are interpreted as being emplaced at the subglacial zone because of the presence of significant shearing and their stratigraphic position on top of highly-deformed strata. Different from unit 1-A, these diamictites were formed subglacially when an advancing glacier overrode and homogenised pre-existing unconsolidated deposits (e.g. Hart 1995). Besides generating subglacial till, this process also deformed the underlying strata and

developed folds, shear planes and thrust surfaces containing slickensides. Such considerations about glaciotectonics are better discussed in the section below.

3.5.2 Ice-marginal association (proximal grounding line-fan deposits)

The amalgamated, coarsening-upward, sandy-gravelly sedimentation intervals that compose almost the whole bulk of middle and upper portions of unit 1-B contains facies compatible with high energy sedimentation processes, such as density flows (hyperconcentrated-to-concentrated) and energic bedload-dominated currents (Table 1). Sets of current-rippled fine- to medium- grained sandstones strata generated by unidirectional tractive flows under lower flow regime occur in between these high energy-derived beds, indicating temporal variation in flow energy. Vertical and downstream rapid facies change in grain-size demonstrate a progressive character change downflow of underflows due to flow deceleration, decreasing sediment concentration and expansion from a confined to an unconfined state in a subaqueous environment (Mulder and Alexander 2001, Russel and Arnott 2003).

Differently those laterally extensive subglacial soft-sediment intraformational surfaces containing grooves, ridges and flutes developed on diamictites of unit 1-A, we reject the subglacially-formed hypothesis for the observed intraformational soft-sediment grooved/striated surfaces over sandstones and conglomerate beds in this facies association. Otherwise, the surfaces are interpreted as iceberg-keel scour marks (IKSM) due to: (i) their laterally-restricted distribution of grooves and ridges; (ii) the presence of marginal berms; (iii) the presence of small-scale slumped and striated sandstone lobes in between the main grooves; (iv) the fact that they occasionally occur on non- to slightly-deformed sandstone and conglomerate beds (e.g. Woodworth-Lynas and Dowdeswell 1994, Eyles *et al.* 2005). Such structures are more common in the stratigraphic record of glaciated basins than previously thought and recently have been documented and

reanalyzed over sandy strata in Paraná Basin (Santos *et al.* 1992, Vesely and Assine 2014, Rosa *et al.* 2016, Fallgatter and Paim 2017, Assine *et al.* 2018).

Accordingly to the rapid downstream facies-change, the presence of IKSM and outsized clasts embedded in well-sorted sandstones, as well as the combination of coarse-grained facies emplaced by density flows and tractive currents, a fluvial or subaerial origin for this facies association is no took into account. Instead, it is related to a deposition within a water body in the form of coarse-grained grounding-line fans fed by sediment-laden meltwater flows from the mouth of englacial/subglacial tunnels placed in the grounding zone of a temperate tidewater calving glacier margin (Eyles *et al.* 1985, McCabe and Eyles 1988, Powell 1981;1990, Powell and Alley 1997, Lønne 1995). Corresponding grounding-line fan deposits have been described and analyzed in detail in the Itararé Group and in other gondwanic late Paleozoic glaciated basins elsewhere and consist in a useful horizon to diagnose glacial cycles since they evidence ice-margin advances in between glacially-influenced successions (e.g. Henry *et al.* 2012, Koch and Isbell 2013, Aquino *et al.* 2016, Mottin *et al.* 2018).

In addition to the sediment budget from meltwater flows, grounding-line fans tend to be wider and thicker as well as their development is facilitated during episodes of stability or quasi-stability of the tidewater ice-margins, when the grounding-zone stagnation give conditions to aggradation of coarse-grained facies (Boulton 1986, Dowdeswell *et al.* 2015). The analyzed sandy diamictite facies (F3) are attributed to have been generated at the most proximal area in relation to the tunnel stream mouth where meltwater flow velocity and sediment load are higher (i.e. zone of flow establishment; Powell 1990, Hornung *et al.* 2007). In a vertical section, the location of these density flow-driven facies is related to lateral shifts in the tunnel mouth positions with time and to the grounding zone drift due to low-time span advance/retreat episodes during grounding-line fan formation (Batchelor and Dowdeswell 2015, Dowdeswell *et al.* 2015). The grounding-line fan stratigraphic record

discussed herein shows a general upward increase in grain-size and in the amount of sandy diamictite facies, suggesting a progradation of the proximal ice-marginal system associated with a main ice-margin advance episode containing low-time span advances and retreats phases (Ingólfsson 1987, van der Wateren 1994, Lønne 1995). implies in ice-marginal sediment squeeze occurring contemporaneously to the grounding-line outwash aggradation, thus generating push-morainal bank complexes (Powell and Molnia 1989, Powell and Domack 2002, Ashley *et al.* 1991, Hunter *et al.* 1996, Lønne *et al.* 2001).

3.5.3 Proglacial association (distal grounding-line fan deposits)

In contrary to the other discriminated facies association, this one was not documented in previous works. Its depositional characteristics are poorly preserved at most places due to subsequent imposed soft-sediment deformation. The strata that composes the bulk of unit 1-B lower and also occur at the top of unit 1-B middle were generated by an assembly of processes that allows to interpret a deposition at the proglacial zone of grounded temperate tidewater glacier and correspond to distal settings of grounding-line systems (Boulton and Deynoux 1981, Molnia 1983, Eyles *et al.* 1985, Powell and Domack 2002). The main characteristic of this association is the predominance of cm- to dm-thick interbedding of outsized clasts-bearing, muddy and sandy (fine-grained) facies, which are attributed to have been generated mainly by low-energy sedimentation processes (Table 1), such as: (i) low-energy tractive currents; (ii) settling of suspended fine sediment from hypopycnal plumes emanated from ice-marginal tunnels; and (iii) rainout of iceberg-rafted debris (IBRD). Concomitant with the deposition of these low-energic facies, gravity-driven resedimentation processes ranging from a hyperconcentrated-to-concentrated to a turbidity current character (*sensu* Mulder and Alexander 2001) are also interpreted to being formative mechanisms of this facies association.

Diverse depositional processes operating at this zone produce facies with textural and structural similarities that, sometimes, are difficult to been attributed to a formation mechanism. For instance, detailed research concerning lithofacies description and formative processes in modern and past proglacial environments result in diverse hypothesis for non-glaciogenic subaqueous mudstones, rhythmites and diamictites emplacement (e.g. Eyles and Lagoe 1990, Dowdeswell *et al.* 1994;2000, Smith and Andrews 2000, Isbell 2010, Henry *et al.* 2012, Bussert 2014, Fleming *et al.* 2016). By outcrop-scale detailed analysis of the textural and structural aspects, likewise facies relationships with overlying and underlying facies, some considerations about depositional processes of observed non- or slightly-deformed facies can be done.

Gravity-driven resedimentation processes are common events in grounding-line systems at tidewater termini glaciers giving rise to a wide range of density flow deposits. High sedimentation rates creating slope over-steepening, iceberg calving impacts and glacier-squeeze are the main factors that contribute to the destabilization of the sediment pile at grounding-line fans (Eyles *et al.* 1985, Powell and Molnia 1989, Nemec 1990, Powell and Domack 2002). On other hand, generation of hypopycnal plumes are conditioned by meltwater flows at ice-marginal subglacial/englacial tunnel stream mouths that generate coarse-grained facies at the grounding-line zone. Most of ejected fine-grained fraction then is transported upward in the water column when flow velocity drops and give rise to an overflow plume that carry fine-grained sand and mud through towards the more distal portions proglacial zone (Powell 1990). This process is distinct to subaqueous environments, however is facilitated to occur in a glaciomarine environment due to lower-density fresh meltwater and higher-density salty seawater contrast (Boulton and Deynoux 1981, Powell and Molnia 1989). IBRD rainout is a common process responsible for sediments of all grain sizes dispersion in the subaqueous environment which is in contact with tidewater calving termini of a grounded temperate glacier (Powell and Domack 2002).

The muddy and sandy muddy, outsized clast-bearing, massive to faint-stratified facies (i.e. sandy mudstones and clast-rich to clast-poor diamictites), as well rhythmically laminated facies that occur interbedded with fine-grained rippled sandstones can be argued as a product of rapid settling of outwash hypopycnal plumes sediment plus IBRD rainout, or as low-magnitude gravity-driven resedimented deposits. Processes of this nature occur concomitantly at the distal grounding zone sediment accumulation zones and the resulted deposits are a function between their dominance over other processes (Eyles *et al.* 1985).

The sandy to intermediate, clast-poor diamictites and massive sandstones placed at the top of unit 1-B lower at locality 16 are interpreted as a product of resedimentation by low-magnitude slumps at distal zones of grounding line fans. The fact that their matrix is partly heterogeneous with remnants of current-ripples displaced by step faults are suggestive of slumps (Alsop and Marco 2011; 2014), differently to the proximal grounding-line fan massive sandy diamictites interpreted as underflow meltwater-fed products. These facies contain tabular sharp basal contacts and often grade upwards to better-sorted and current-rippled sandstones. Such relation demonstrates a downflow transformation where finer particles enter in a diluted support and deposit lower-flow-regime-generated sandstones on grain-to-grain supported massive facies as flow decelerates and loses sediment transport capacity (Mulder and Alexander 2001). Tabular sets of current-rippled sandstones with downflow macroforms accretion in between those facies marks the temporal domination of low-energy tractive currents.

Mm- to cm-thick heterolithics mud/sand laminae and lenses (rhythmites) are suggestive of deposition by underflow turbidity currents associated with settling of hypopycnal plumes with minor iceberg melting and IBRD rainout since they display an assemblage of characteristic like: (i) minor truncations between laminae sets and mudstone rip-up clasts indicating erosion between each turbidity flow; (ii) mudstone laminae are thicker and contain embedded clasts of very coarse sand to granules, occasionally

deforming the laminae; (iii) close association with fine-grained climbing-rippled sandstones with mm-thick mud drapes on foresets; and (iv) occurrence of small current-ripples in the sand laminae (e.g. Walker 1965, Sturm and Matter 1978, Stow and Shanmugam 1980, Thomas and Connell 1985, Molnia 1989). Taking into account, we argue against the lacustrine seasonally-induced varve formation by sediment decantation (Brauer 2004, Anderson and Dean 1988, Fitzsimons and Howarth 2018) as the depositional mechanism for these rhythmites.

The faint stratification of some intermediate clast-rich massive diamictites are defined by 1 cm-thick mudstone-dominated continuous laminae which are better sorted than the surrounding matrix. Such diamictites are suggestive of deposition at distal zones of the tidewater termini by a combination of hypopycnal plume settling with IRDB rain-out in which mudstone laminae were deposited during fluctuations in the balance between mud supply and IRDB rainout (Powell 1994).

Heterolithics facies generated by the combination of turbidity flows, settling of fines and IRDB rainout grade upward to massive sandy mudstones with dispersed clasts up to granule-size. It manifests a progressive minor contribution of underflow resedimentation and the prevalence of hypopycnal plume settling followed by IRDB rain-out (Eyles *et al.* 1985). Sandy mudstone beds are up to 30 cm-thick and interbedded with current-rippled fine-grained sandstone layers no thicker than 15 cm with abrupt basal and upper contacts. This alternation is attributed to the occurrence of low-energy tractive currents during at some time concomitant with mud and fine sand settling. At some level, the sandy massive mudstones grade to a 25 cm-thick layer of a massive sandy, pebble-rich, diamictite that passes upward again to the massive sandy mudstones. This IBRD-rich layer evidences a temporal dominance of IBRD rain-out over settling of hypopycnal plumes (Powell and Molnia 1989, Streuff *et al.* 2017). In temperate regimes, sediment budget by meltwater input and mud deposition tends to prevail over iceberg rainout in the proglacial zone, such

situation can invert when the amount of iceberg enhances due to high-rate calving episodes or decrease in meltwater discharge (Powell 1981, Pfirman and Solheim 1989, Powell and Domack 2002).

Definition of facies formative processes that occur in the proglacial zone are essential since they help to interpret the proximity of the grounding-line in the proglacial zone (Powell and Cooper 2002). Whereas unit 1-B lower stacking pattern and grain-size distribution suggest a progradation from a mud-dominated distal zone to a slumped sandy proximal zone, the unit 1-B middle shows the opposite, grading upwards from a current-rippled sandy fine-grained interval to a mud and IBRD-rich interval (Fig. 3A-B). Also, the lack of varve deposits *sensu stricto* and abundance of deposits generated by settling of buoyant hypopycnal plumes seems likely to a glaciomarine setting, contradicting the glaciolacustrine environment proposed by Vesely *et al.* (2015).

3.6 GLACIOTECTONICS

Although with variable intensities and structural styles, penecontemporaneous, soft-sediment deformation is present throughout the studied succession. Distinction between deformation driven by mass-transport and glaciotectonics is a difficult task because the structural assemblage can be quite similar (Eyles *et al.* 1985, Visser *et al.* 1984, van der Wateren 2002). In our study case, evidence for a glaciotectonic origin include a close association with glaciogenic features like striated surfaces, striated and bullet-shaped clasts, ice-rafted outsized clasts and ice-keel scour marks and vertical profiles that show an upward increase in deformation (Hart *et al.* 1990) that differ from basal shear zones developed beneath mass-transport deposits (e.g. Hart and Roberts 1994, van der Wateren 2002). The overall consistency of measured structures (Fig. 3C) suggests highly confined stress fields for deformation, a characteristic that differs from slides and slumps where soft-sediment deformational structures are often randomly distributed due to unconfinement and the influence of submarine topography (Hart and Roberts 1994, Dykstra *et al.* 2011). In Addition, the exorbitant predominance of structures generated under compressional and simple shear regimes over extensional regime-induced structures, which are more likely to mass-transport deposits, also seems to rule out slumping as the responsible for the observed deformation (Visser *et al.* 1984, Martinsen 1994).

Except for small step faults disposed internally to tabular diamictite beds (F4), interpreted as result of slump processes in a grounding-line fan slope, the structures described herein are interpreted to have been generated by stress directly transmitted from advancing glaciers onto unconsolidated to semi-consolidated being thus a product of glaciotectonics (Aber *et al.* 1989, van der Wateren 2002, McCarroll and Rijsdijk 2003, Phillips 2018). The assembly of glaciotectonic structures allowed the recognition of intervals deformed in simple-shear-dominated subglacial settings as well as under compressional regime at the glacier margin (McCarroll and Rijsdijk 2003). The internal architecture and

styles of push-moraines is high variable and depends mainly on the foreland rheology and glaciologic conditions at ice-margin/sediment interface (Bennett 2001). Although a not deeper evaluation on push-moraine anatomy can be made, the assembly of glaciotectonic structures support some brief considerations on the styles of the three push-moraines identified in the ice-complex.

In addition to diamictites of unit 1-A emplaced at subglacial zone during a glacier advance on bedrock, part of strata of unit 1-B lower as well the muddy diamictite place on top of unit 1-B upper are credited to have been generated at the subglacial zone and acted as the basal deforming layer (Evans *et al.* 2006, Menzies *et al.* 2018). A typical idealized vertical sequence/continuum of subglacially simple-shear-deformed sediments during a glacier overriding, where strain rates enhance towards the glacier sole and there is a transition from glaciotectonites to a deformation till (Hart *et al.* 1990, Hart and Boulton 1991, Benn and Evans 1996, van der Wateren 2002), fits in the observed sequence of lower portion of unit 1-B placed at locality 2 and correlated to diamictites exposed at locality 12. At this location there is an upward transition from a bottom zone dominated by rootless isoclinal folds, passing trough a zone dominated by subhorizontal shear planes in a heterogeneous matrix with boudinaged and disrupted sandier layers towards homogenised diamictites on top with a high-density of subhorizontal anastomosing shear surfaces. An exposure at locality 16 of unit 1-B lower contains low deformation rates where tilted strata disposed in gentle to open folds and somewhen boudinaged and cut by reverse faults are indicative that part of unit 1-B lower was deformed in ice-marginal settings, corresponding to distal zones of a push-moraine.

The whole unit 1-B middle are credited to be deformed at the ice-marginal zone during an episode of ice advance and represents the distal portions of the deformed foreland. Considerations about this push-moraine can be done at localities 3 to 5 where grounding-line sandy-gravelly and proglacial fine-grained deposits show low-accentuated

folding and thrusting. The gentle and open folds observed at these outcrops are parasitic folds of mega-scale synclines and anticlines. Subhorizontal truncation surfaces in between the sandy-gravelly deposits that truncate sets of folded strata, can be argued as product of syn-glaciotectonics during grounding-line outwash aggradation (van der Wateren 1994, 1995) or mega-scale shear surfaces related to the nappe style compressional deformation generated by ice lobes (Kluiving 1994, van der Wateren 1995). At this model, nappes are internally slightly deformed and bounded by simple shear-dominated shear zones. Imbricated low-angle thrusting in minor scale occur at the base of some names especially in their distal extremities (Bennett 2001). The rheology of deformed material plays a role on the deformation degree. The proglacial fine-grained facies bedding and internal depositional structures are gently-folded, thinned and thickened, however still preserved with exception made of some horizons placed at the contact with sandy-gravelly strata and in between fine-grained interbedding where facies with higher mud content contain a high-density of subhorizontal shear mm- to cm-sized shear surfaces and heterogeneous matrix containing remnants of sedimentary structures. In indicates simple-shear dominated shear horizons and intrastratal displacement facilitated by bedding discontinuities associated with stratal composition contrasts and facies higher mud content (van der Wateren 1985, Murray 1994).

The push-moraine that is materialized in deformed grounding-line fan deposits of unit 1-B upper is more likely related to a thrust-fold dominated style (Croot 1987) and has a more complex assembly of glaciotectonic structures since it was overridden. The sandy-gravelly bulk of this grounding zone deposits does not allow significant intrastratal discontinuities and high mud content, being this imposed deformation in more brittle regime (Bennett 2001). High shear strain is confined inside that bound some non- to moderately-deformed sets of sandy-gravelly strata. These thrusts are sometimes rooted in the base of the sandy-gravelly association and possibly related to a rooting in a décollement surface

that bases the whole push-moraine (Boulton *et al.* 1999). Folds related to thrusting are common and range from close to tight and their show a more asymmetric profile.

Homogeneous sheared muddy diamictites placed as mega-slabs in between the top strata of unit 1-B upper at locality 13 shows slickensided sheared contacts with surrounding strata interpreted as grounding-line fan deposits. These diamictites are also attributed to a basal deforming layer and its emplacement as slabs due to transmitted ice-stress is common in push-moraines at the subglacial to ice-marginal transitional zone (Boulton 1996, van der Wateren 2002). On other hand, at outcrops corresponding to the top strata of this unit at the railroad track (localities 9 to 10), there is a superimposition of simple-shear-dominated structures over compressional-deformed strata that progressively fades away the original bedding upwards to a homogeneous intermediate massive diamictite with a basal diffuse contact. Such structures are more pervasive in sandy diamictites layers than in well-sorted sandy strata. Also, normal faulting associated with boudinaged of current-rippled sandstone layers occur and are related to subglacial simple shear. Brittle fractures are correspondent to some observed described fractures in Cenozoic deposits (Rijsdijk *et al.* 1999;2010) and related to upward water-scape (i.e. hydrofracturing) forced by subglacial shearing on water-saturated sediments. At Witmarsum locality, few outcrops of this unit are available, and these sandy-gravelly strata is poorly deformed and capped by a muddy sheared diamictite. No relationship between facies were possible, but we conclude that this location represents the distal portions of the push-moraine complex before being overridden by the glacier.

3.7 GLACIAL CYCLICITY AND ICE-FLOW PATTERNS

Considering the vertical changes in facies association and deformation patterns, as well as glaciers kineto-indicators, a glacial cyclicity can be recognized in the studied interval, in which three major glacial cycles of advance and retreat at the lowermost portion of Itararé Group can be defined (Fig. 3A). A graphic representation of these three cycles is shown in Fig. 12.

The known age for the Lagoa Azul Formation in Paraná state is based on palynomorph analysis in a local (Kipper 2014, Kipper *et al.* 2017) and basinal scale (Souza 2006), correspond to the *Ahrensisporites cristatus* biozone and is settled as late Bashkirian to late Moscovian (around 318 – 307 Ma) (Fig. 1). The ice-contact complex corresponds to the lower one third of the Lagoa Azul, suggesting that was formed by a shorter period of time. The age of these deposits relies in a time of major estimated ice volumes during the LPIA, which can be interpreted as the LPIA glacial maximum as suggested by late Visean – lower Guadalupian isotopic analysis on tropical carbonates in China (Chen *et al.* 2016). Taking into in account, the glacial cycles discussed below are related to higher-frequency cycles (or subcycles) than previously defined glacial cycles to Itararé Group (e.g. França and Potter 1988, Vesely and Assine 2006) with a similar time span of those subcycles defined by Buso *et al.* (2017) to the uppermost Itararé Group strata (Taciba Formation).

3.7.1 Glacial cycle 1 (GC1)

During the glacial cycle 1 (GC1), a warm-based ice lobe advanced northward and abraded the underlying Furnas Formation and the Precambrian basement, carving striated pavements on bedrock. A sheet of sandy tillites (unit 1-A) was deposited subglacially just on this late Devonian-Bashkirian nonconformity at the outer subglacial zone. The modification of the original sedimentary pile by Phanerozoic reactivations of major basement fault systems (Lancinha Shear Zone; Fig. 2) (Sadowski 1991, Castro *et al.* 2014) and by

Mesozoic uplifting of the Ponta Grossa Arch (Strugale *et al.* 2007) hampers to deduce if there was a topographic control on glacier flow as has been documented in other parts of the Paraná Basin (e.g. Fallgatter and Paim 2017). However, the flat surfaces associated with the basal unconformity points out to a glacier unconstrained by topography, thus excluding fjord or ice-stream settings for this ice lobe.

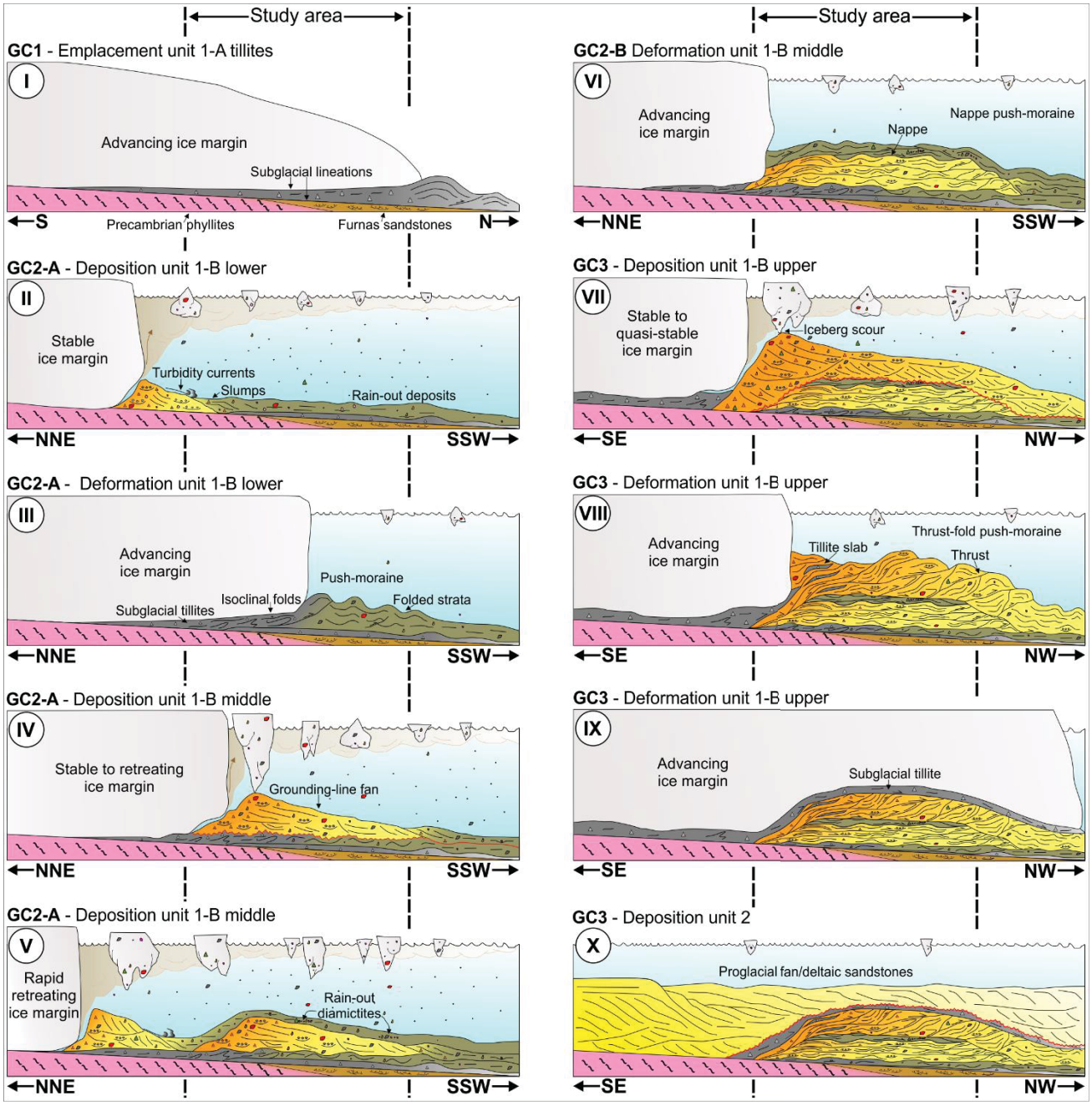

Figure 12 – Inferred evolution of the ice-complex at Balsa Nova region during the three glacial cycles discussed herein.

If the glacier advanced on emerged land or into a subaqueous environment (marine/lacustrine) is still unclear. Trosdtorf *et al.* (2005) suggested the latter and admitted a rapid glacier retreat followed by meltwater-fed deltaic progradation (correlated herein to unit 1-B lower). Vesely *et al.* (2015), on the other hand, interpreted that these deltaic sediments filled a small moraine-dammed lake that developed in front of a retreating terrestrial glacier. However, our paleocurrents from the proglacial deposits that immediately overlie the tillite indicate sediment transport towards SW (Fig. 3C) and a glacial source located to NE, meaning that the water body was not filled by sediment derived from the retreating ice-margin of the GC1 ice lobe that produced the basal tillite. This also evidence an apparent lack of deglacial deposits directly derived from this northward advancing ice lobe in this area suggestive of a rapid glacier retreat (Boulton 1990, Dowdeswell *et al.* 2015) followed by a rapid marine incursion that generated accommodation space for the deposition of subsequent units.

3.7.2 Glacial cycle 2 (GC2)

The deposits associated to this glacial cycle are stratigraphically above the basal tillite and belong to the lower and middle portions of unit 1-B. This glacial cycle 2 (GC2) consists of a major cycle comprising two subordinated cycles (GC2-A and GC2-B) of minor ice-margin fluctuations of the wet-based, tidewater termini ice lobe (see stages II to VI; Fig 12).

The establishment of fine-grained proglacial deposition at the distal portions of grounding-line fans evidences the beginning of GC2-A sedimentation within a marine environment just after the southward retreat of GC1 ice lobe. Paleocurrents and the coarsening-upward pattern of unit 1-B lower suggest a progradation of proglacial systems towards SW (243°; Fig. 3C) relatively far from a grounded, wet-based, tidewater ice-margin placed farther to the NE, evidenced by occurrence of IBRD in these deposits. This

progradation is interpreted to have operated during a constant ice-margin advance, which culminated with the glacier overriding most of the proglacial facies, as well deforming some portions at ice-marginal settings giving rise to push-moraines. Favor this interpretation the fact that paleo-ice flow deduced from subglacial glaciotectonic structures (i.e. shear planes and isoclinal folds) is towards the WSW (260°; Fig. 3C), roughly parallel to sediment transport prior to deformation.

A retreat phase towards ENE marks the end of the GC2-A and its record is materialized in the deglaciation deposits of unit 1-B middle. Paleocurrents from proglacial and grounding-line fan deposits have a mean vector towards SW (241°; Fig. 3C), which is consistent with a meltwater source located to ENE. The sandy-gravelly grounding line-fan deposits exhibit an overall coarsening-upward pattern and internal facies variation interpreted as a consequence of temporal changes in meltwater discharge during a phase of stability or quasi-stability of the grounding-zone during retreat. The sudden break in the transition from the basal grounding-line fan deposits to the upper fine-grained proglacial interval records a backstepping of the grounding-line fan likely due to a rapid change from stabilized to retreating ice-margin behavior.

The subsequent deformation of deglacial deposits of GC2-A are related to shear imposed by ice-push during a renewed ice lobe advance. This advance event marks the onset of GC2C-B which gave rise to a push-moraine characterized by folded strata truncated by mega-scale subhorizontal shear surfaces comparable to the nappe model of van der Wateren (1994, 1995). The stereographic analysis of folded strata and shear surfaces attributed to GC2-B advance (260° - 273°; Fig. 3C) evidences a westward deformational vergence similar to GC2-A. Therefore, this episode can be related with a readvance of the same ice-margin associated with GC2-A, implying in minor fluctuations of a west-southwestward flowing ice lobe during the GC2.

3.7.3 Glacial cycle 3 (GC3)

The ice-retreat record of GC2-B is not preserved and it is believed to have been a combined result of low rates of deposition and high erosion rates during the onset of glacial cycle 3 (GC3). The initial phase of the third cycle is recorded by the widespread proximal grounding-line fan deposits of upper unit 1-B, which are placed on a prominent unconformity that locally cut underlying deposits of GC1 and GC2 and touches the Precambrian basement. The unconformity was probably generated by vigorous meltwater flows that highly-scoured the unconsolidated substrate (e.g. boulder-sized rip-up clasts; Fig. 9C) and sourced high amounts of glacial debris to build a large grounding-line fan system at the margin of a temperate ice lobe (Ashley *et al.* 1991, Hunter *et al.* 1996). A progradation of this fan to NW is indicated by the coarsening-upward pattern and a paleocurrent mean vector trending 322° (Fig. 3C), implying in an ice-margin placed to SE. Phases of ice-margin stability associated with calving probably allowed the generation of a thick and laterally extensive sandy-gravelly succession that are widespread in the area.

The coarsening-upward pattern of facies and the vergence of glaciotectonic structures (Fig. 3C) indicate a glacier advance to NW that progressively deformed the grounding-line deposits. This deformation first involved compression due to ice-push at ice-marginal settings engendering a thrust-fold dominated push-moraine with tillite slabs in the proximal zone and subsequently a superimposed simple shear subglacial deformation due to progressive glacier override the push-moraine complex.

The simple-shear-dominated subglacial deformation indicates that the glacier movement was controlled mainly by deformation of underlying deposits. These deposits plus the subglacial tillites are widespread and reach the northwesternmost portion of the study area. This suggests that, contrary to previous interpretations (e.g. Vesely *et al.* 2015), that the ice margin advanced far beyond the area of the present study, probably reaching more internal zones of the basin during GC3 glacial maximum.

The retreat of this grounded, wet-based ice lobe and the deglaciation phase of GC3 are recorded by the glacially-influenced, undeformed, proglacial fan to deltaic sandstones that are just above the ice-contact complex by a widespread angular unconformity. These sandstones have paleocurrents to the northwest and contain intraformational iceberg scours indicating that the ice margin was still in contact with the water body (Vesely and Assine 2014, Vesely *et al.* 2015). The fact that the analyzed glaciogenic interval is directly overlaid by proglacial fan to deltaic deposits and not by deep-marine deposits such as black shales and submarine slope mass-transport (e.g. Puigdomenech *et al.* 2014, Aquino *et al.* 2016, Fallgatter and Paim 2017) suggests that the ice-complex was generated in a relatively shallow marine environment, mainly controlled by fluctuations of a grounded tidewater glacier.

3.8 PALEOGEOGRAPHIC IMPLICATIONS

During the Early Pennsylvanian the South Pole was over Antarctica and the eastern margin of the Paraná Basin was placed on 45-50° paleolatitudes (Powell and Li 1994) which is similar to the latitudes of the maximum extent of ice lobes derived from Pleistocene ice sheets in North America (Ehlers and Gibbard 2007).

Based on modern views of LPIA evolution that assumes smaller ice centers than traditionally inferred (Isbell *et al.* 2003, Fielding *et al.* 2008, Isbell *et al.* 2012), paleogeographic reconstructions point out for the presence of the Windhoek Ice Sheet (WIS) as a source of ice masses that carved glacial valleys in western Namibia (Frakes and Crowell 1970, Martin 1981, Visser 1987) and reached the eastern border of the Paraná Basin (Santos *et* al. 1996, Vesely *et al.* 2015, Fallgatter and Paim 2017). Since the glaciers discussed herein do not possess evidence of topographic control as well as sedimentation in fjord or ice-stream settings (Clark and Stokes 2005, Hambrey and Glasser 2012), our interpreted glacial cycles are related to the marginal portions of ice lobes possibly fed by Namibian ice-streams (Patterson 1997;1998) that represent WIS maximum extent at this region during the late Bashkirian-Moscovian LPIA onset in eastern Paraná Basin.

The time frame between and during each of the glacial cycles as well as the amount of ice lobes responsible for the ice-complex deposition is uncertain because of the lack of ice-masses track and high-resolution chronostratigraphy and provenance analysis. Vesely *et al.* (2015), by studying the deposits examined herein, postulated that the deposition of the Lower Pennsylvanian basal strata in Paraná State was influenced by two separate ice lobes referred to as Southern Paraná Ice Lobe (SPIL) and Northern Paraná Ice Lobe (NPIL). According to this model, the area of the present study stayed under the influence of SPIL, which behaved as a fluctuating ice margin moving on emerged land towards N and NW (correlated herein to GC1 and GC3) and the NPIL took place in Ventania region about 130 km farther north.

However, the results of the present study suggest a more complex scenario, involving the interaction of multiple advance and retreat phases of likely distinct ice lobes in order to explain the stratigraphic complexity and changes of ice-flow direction with time. Taking into in account, we propose a model to Paraná Basin LPIA onset during Lower Pennsylvanian glacial maximum based on previous paleogeographic reconstructions and recent published data in analogy with the outlet ice lobes behavior of Northern Hemisphere Pleistocene ice sheets (Fig. 13).

Erosional features placed on the Itararé basal nonconformity and basal tillites (Rosa *et al.* 2016) as well as paleocurrent recorded in lowermost Itararé Group (Vesely *et al.* 2015) in regions farther north show a strong general NW ice-flow arrangement for the WIS ice lobes. GC1 and GC2 ice-flow patterns at Balsa Nova region deviate from this regional framework evocating that can be a consequence of the radial lobate termini of ice lobes (e.g. Evans *et al.* 2008, Glasser *et al.* 2008, Kehew *et al.* 2012). Based on this, the GC1 ice lobe corresponds to SPIL that flowed northwestward from WIS on emerge land and only its marginal northward ice-flow pattern is record at the study area (Fig. 13A), The GC1 rapid ice lobe retreat was followed by a marine incursion and the ice-complex strata stayed under influence of NPIL during GC2 which is registered at Balsa Nova region with a west-southwestward ice-flow direction (Fig. 13B). The NPIL can be argued also as the responsible for deposition in Ventania area and by the generation of subglacial intraformational striated surfaces over basal diamictites in southern São Paulo state (Caetano-Chang *et al.* 1990).

U-Pb detrital zircon ages of grounding-line fan deposits of unit 1-B upper (i.e. relative to GC3) at Bassani sand pit demonstrate a major local-source contribution of Neoproterozoic zircons derived from Precambrian granitic rocks placed some kilometers SE of Balsa Nova (Griffis *et al.* 2018a) expressive that GC3 was under influence of a readvance of SPIL (Fig. 13C).

In addition to the influence of NPIL and SPIL on sedimentation in eastern Paraná Basin, the Kaokoveld Ice Lobe (Frakes and Crowell 1970, França and Potter 1988, Santos *et al.* 1996) is also invocated for the areal scouring and shaping streamlined bedforms on Precambrian basement in São Paulo state (Almeida 1948, Amaral 1965, Rocha-Campos *et al.* 1968, Viviani and Rocha-Campos 2002, Pérez-Aguilar *et al.* 2009) during the LPIA onset in eastern Paraná Basin.

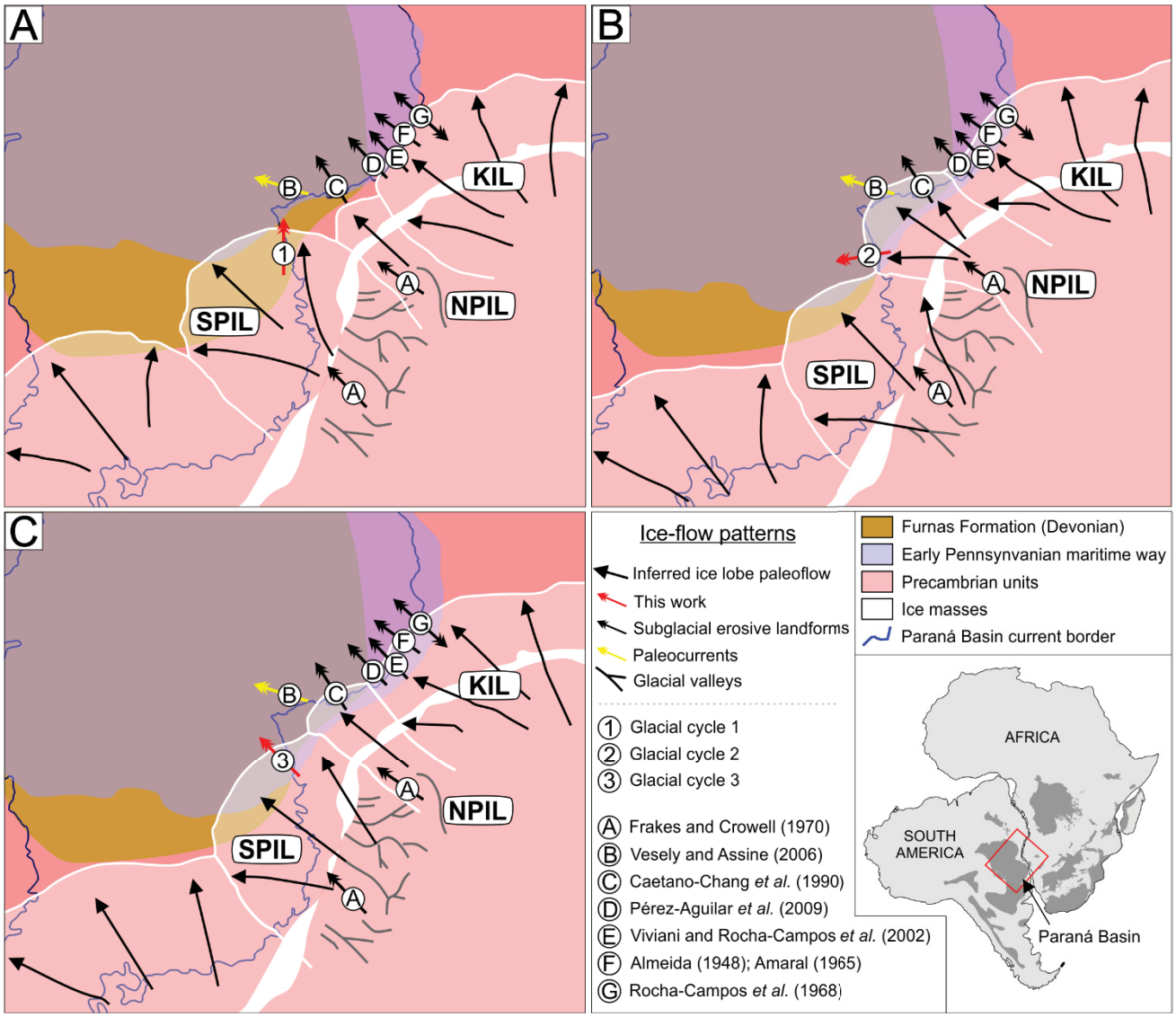

Figure 13 – Postulated paleogeographic model for the Lower Pennsylvanian LPIA onset at eastern margin of the Paraná Basin according to **(A)** glacial cycle 1, **(B)** glacial cycle 2, **(C)** glacial cycle 3. Paleogeographic map location shown in reconstructed South America and Africa during Gondwana with the main LPIA basins. KIL = Kaokoveld Ice Lobe; NPIL = Norther Paraná Ice Lobe; SPIL = Southern Paraná Ice Lobe. Areal distribution of Devonian units obtained from isopach map in Milani and Ramos (1988). Maritime way based on isopach maps of Lagoa Azul Formation from Santos (1987) and França and Potter (1988).

Another possible ice center that emanated ice masses to Paraná Basin margins during the Early Pennsylvanian was placed over a region that comprehends southern Brazil, Uruguay, easternmost Argentina and southwesternmost Africa (Rosa *et al.* 2016, Fallgatter and Paim 2017, Assine *et al.* 2018, Griffis *et al.* 2018a), thus being related to the same source of younger Uruguay Ice Lobe responsible for generating subglacial features with a similar N-S trend during late Carboniferous to early Permian (Tomazelli and Soliani 1982;1997, Assine *et al.* 2018). A topographically-controlled Early Pennsylvanian ice center placed at this region is plausible since there is a prolonged late Devonian – late Pennsylvanian sedimentation gap consequence of the Chañic (Eo-Hercynian) orogeny at Panthalassa gondwanic margin related to Gondwanides (López-Gamundí and Rossello 1993;1998, Milani and de Wit 2008). Glaciogenic to glaciomarine sedimentation record in southern Paraná Basin and Sauce-Grande basin started in late Pennsylvanian (di Pasquo *et al.* 2008, Griffis *et al.* 2018b) as accommodation gradually moved southwards due to eustatic rise (Holz *et al.* 2010, Vesely *et al.* 2017) suggesting that continental glaciers were active and restricting deposition in that region during Early Pennsylvanian (González-Bonorino and Eyles 1995).

Subsequently to the glacial cycles discussed herein, the end of Lagoa Azul Formation deposition eastern rim of the basin, near the Moscovian-Kasimovian boundary, is portrayed by a relative sea level rise evidenced by the transition to deep-marine sedimentation. The sea level rise can be argued as a consequence of major ice lobes retreat; however, they were still in contact with the marine environment, evidenced by presence of iceberg-rafted debris and iceberg keel scour marks in these deposits (Vesely and Assine 2006, Vesely *et al.* 2015).

3.9 CONCLUSIONS

By combining sedimentology and structural analysis of a lower Pennsylvanian ice-contact complex belonging to the lowermost Itararé Group in Balsa Nova region, eastern Paraná Basin, some conclusions can be enumerated concerning late Paleozoic glaciodynamics and paleogeography in this region of western Gondwana:

(1) Three facies association corresponding to subglacial tillites, ice-marginal (proximal grounding-line fan) and proglacial (distal grounding-line fan) are recurrent in four defined informal stratigraphic units occurring in the base of the Lagoa Azul Formation. Such facies association were deformed in subglacial and ice-marginal settings giving rise to subglacial tillite sheets and push-moraine complexes.

(2) The vertical recurrence of facies association and deformed intervals record an advance-retreat glacial cyclicity designated as GC1, GC2 and GC3. Each glacial cycle corresponds to a glacial advance towards north, west-southwest and northwest, respectively.

(3) With exception of subglacial tillites placed in the lower portion, which its environment discussion is still open, the ice-complex was generated under influence of advances of grounded temperate ice lobes with tidewater termini in a glaciomarine environment, what contradict previous interpretations that assumes a glaciocontinental (glaciolacustrine) origin for these deposits. It impacts in an earlier marine incursion during Early Pennsylvanian than previous stipulated.

(4) Glaciotectonic soft-sediment structures are a reliable indicator of ice-flow patterns in between the LPIA strata and mapping of glaciotectonized intervals should be more engaged in order to constrain the LPIA glacier kinematics since the widely employed kineto-indicators are over the basal nonconformity.

(5) This basal interval provides valuable information about LPIA ice-flow patterns and the interaction of more than a single glacier in deposition of a thin interval. We

strongly encourage future detailed research on provenance analysis and mapping of ice-tracks to constrain source-area and glaciers timing during the LPIA onset in Paraná Basin as well as in other gondwanic basins.

4 CONSIDERAÇÕES FINAIS

O estudo em detalhe do intervalo majoritariamente glaciogênico situado no sudeste do estado do Paraná trouxe à tona algumas questões referentes aos primeiros estágios de sedimentação e da ação glacial neopaleozoica na Bacia do Paraná.

A maioria das feições utilizadas para a definição do sentido de paleofluxo glacial e que registram a presença direta de geleiras estão situadas sobre a discordância que embasa o Grupo Itararé, resultando no fato de que os ciclos glaciais e sentidos de fluxo das geleiras neopaleozoicas são definidos indiretamente a partir da análise da ciclicidade dos depósitos marinhos glácio-influencidos e pela análise de paleocorrentes. De outro lado, a análise glácio-tectônica realizada pôde constatar que a orientação de estruturas deformacionais e a distribuição vertical dos estilos de deformação é uma poderosa ferramenta que, combinada à análise estratigráfica, permite inferir atributos paleoglaciológicos e distinção de ciclos glaciais de menor escala em eras glaciais pretéritas.

A distinção de três ciclos glaciais de menor escala em um contexto local resultantes da interação de três lobos glaciais com diferentes sentidos de fluxo (N, SSW e NW) durante o máximo glacial da Era Glacial Neopaleozoica sugere um cenário mais complexo do que previamente estipulado e que envolve a interação de mais de um lobo glacial na deposição de uma determinada área de pouca expressão geográfica.

REFERÊNCIAS

Aber J.S., Croot D.G., Fenton M.M. 1989. Glaciotectonic landforms and structures, Springer-Science, 203 pp.

Almeida F.F.M. 1948. A "Roche Moutonnée" de Salto, Estado de São Paulo. *Boletim Geologia e Metalurgia*, **5**:112-118.

Alsop G.I., Marco S. 2011. Soft-sediment deformation within seismogenic slumps of the Dead Sea Basin. *Journal of Structural Geology,* **33**:433-457.

Alsop G.I., Marco S. 2014. Fold and fabric relationships in temporally and spatially evolving slump systems: A multi-cell flow model. *Journal of Structural Geology,* **63**:27-49.

Amaral S.E. 1965. Nova ocorrência de rocha moutonée em Salto, SP. *Boletim da Sociedade Brasileira de Geologia*, **14**:71-82.

Anderson R.Y., Dean W.E. 1988. Lacustrine varve formation through time. *Palaeogeography, Palaeoclimatology, Palaeoecology,* **62**:215-235.

Aquino C.D., Buso V.V., Faccini U.F., Milana J.P., Paim P.S.G. 2016. Facies and depositional architecture according to a jet efflux model of a late Paleozoic tidewater grounding-line system from the Itararé Group (Paraná Basin), southern Brazil. *Journal of South American Earth Sciences*, **67**:180-200.

Arzhannikov S.G., Braucher R., Jolivet M., Arzhannikova A.V., Vassalo R., Chauvet A., Bourlès D., Chauvet F. 2012. History of late Pleistocene glaciations in the central Sayan-Tuva Upland (southern Siberia). *Quaternary Science Reviews*, **49**:16-32.

Ashley G.A., Boothroyd J.C., Borns H.W. Jr. 1991. Sedimentology of late Pleistocene (Laurentide) deglacial-phase deposits, eastern Maine; An example of a temperate marine grounded ice-sheet margin. *In*: Anderson J.B., Ashley G.M. (Eds.) Glacial marine sedimentation; Palaeoclimatic significance, Geological Society of America, Special Paper, 261, pp. 107-125.

Assine M.L., de Santa Ana H., Veroslavsky G., Vesely F.F. 2018. Exhumed subglacial landscape in Uruguay: Erosional landforms, depositional environments, and paleo-ice flow in the context of the late Paleozoic Gondwanan glaciation. *Sedimentary Geology,* **369**:1-12.

Atkins C.B., Barrett P.J., Hicock S.R. 2002. Cold glaciers erode and deposit: Evidence from Allan Hills, Antarctica. *Geology*, **30**(7):659-662.

Attig J.W., Mickelson D.M, Clayton L. 1989. Late Wisconsin landform distribution and glacier-bed conditions in Wisconsin. *Sedimentary Geology*, **62**:399-405.

Batchelor C.L., Dowdeswell J.A. 2015. Ice-sheet groundind-zone wedges (GZWs) on high-latitude continental margins. *Marine Geology*, **363**:65-92.

Benn D.I., Clapperton C.M. 2000. Pleistocene glacitectonic landforms and sediments around central Magellan Strait, southernmost Chile: evidence for fast outlet glaciers with cold-based margins. *Quaternary Science Reviews*, **19**:591-612.

Benn D.I., Evans D.J.A. 1996. The interpretation and classification of subglacially-deformed materials. *Quaternary Science Reviews*, **15**:23-52.

Benn D.I., Evans D.J.A. 2010. *Glaciers and Glaciation*. Hodder Education, London, 817p.

Bennett M.R. 2001. The morphology, structural evolution and significance of push moraines. *Earth-Science Reviews*, **53**:197-236.

Bennett M., Glasser N. 2009. *Glacial geology: ice sheets and landforms*. Wiley-Blackwell, Oxford, 385p.

Berthelsen, A. 1978. The methodology of kineto-stratigraphy as applied to glacial geology. *Bulletin of the Geological Societ of Denmark*, **27**:25-38.

Bigarella J.J., Salamuni R., Fuck R.A. 1967. Striated surfaces and related features, developed by the Gondwana ice sheets (state of Parana, Brazil). *Palaeogeography, Palaeoclimatology, Palaeoecology,* **3**:265-276.

Boulton G.S. 1986. Push-moraines and glacier-contact fans in marine and terrestrial environments. *Sedimentology*, **33**:677-698.

Boulton G.S. 1990. Sedimentary and sea level changes during glacial cycles and their control on glaciomarine facies architecture. *In*: Dowdeswell J.A., Scourse J.D. (Eds.) Glacimarine Environments: Processes and Sediments. Geological Society Special Publication, 53, pp. 15-52.

Boulton G.S. 1996. Theory of glacial erosion, transport and deposition as a consequence of subglacial sediment deformation. *Journal of Glaciology*, **42**(140):43-62.

Boulton G.S., Deynoux M. 1981. Sedimentation in glacial environments and the identification of tills and tillites in ancient sedimentary sequences. *Precambrian Research*, **15**:397-422.

Boulton G.S., van der Meer J.J.M., Beets D.J., Hart J.K., Ruegg G.H.J. 1999. The sedimentary and structural evolution of a recent push moraines complex: Holmstrømbreen, Spitsbergen. *Quaternary Science Reviews*, **18**:339-371.

Braakman J.H., Levell B.K., Martin J.H., Potter T.L. van Vliet A. 1982. Late Paleozoic Glaciation in Oman. *Nature*, **299**:48-50.

Brauer A. 1994. Annually laminated lake sediments and their palaeoclimatic relevance. *In:* Fischer H., Kumke T., Lohmann G., Flöser G., Miller H., von Storch H., Negendank J.F.W. (Eds.) The Climate in Historical Times, Springer, Berlin, pp 109-128.

Buso V.V., Aquino C.D., Paim P.S.G., Souza P.A., Mori A.L., Fallgatter C., Milana J.P., Kneller B. 2017. Late Paleozoic glacial cycles and subcycles in western Gondwana: Correlation of surface and subsurface data of the Paraná Basin, Brazil. *Palaeogeography, Palaeoclimatology, Palaeoecology,* (em impressão).

Bussert R. 2010. Exhumed erosional landforms of the Late Palaeozoic glaciation in northern Ethiopia: Indicators of ice-flow direction, palaeolandscape and regional ice dynamics. *Gondwana Research*, **18**:356-369.

Bussert R. 2014. Depositional environments during the Late Palaeozoic ice age (LPIA) in northern Ethiopia, NE Africa. *Journal of African Earth Sciences*, **99**:386-407.

Caetano-Chang M.R., Oliveira J.P., Brighetti J.M.P. 1990. Pavimento estriado em rochas do Subgrupo Itararé ao longo do Rio Piritubinha, sul do estado de São Paulo. *Revista Brasileira de Geociências,* **20**:333-335.

Campos J.E.G., Dardenne M.A. 2002. Pavimentos estriados do Grupo Santa Fé – Neopaleozóico da Bacia Sanfranciscana, MG. Registro de abrasão glacial do Neopaleozóico. *In:* Schobbenhaus C., Campos D.A., Queiroz E.T., Winge M., Berbert-Born M.L.C. (Eds.) Sítios Geológicos e Paleontológicos do Brasil, 1° ed., Brasilia, DNPM/CPRM – SIGEP, pp. 161-164.

Canuto J.R. 1993. Fácies e ambientes de sedimentação da Formação Rio do Sul (Permiano), Bacia do Paraná, na região de Rio do Sul, estado de Santa Catarina. Tese de Doutorado, Instituto de Geociências, Universidade de São Paulo, 164p.

Canuto J.R., Santos P.R., Rocha-Campos A.C. 2010. Fácies e associações de fácies de diamictitos do Subgrupo Itararé (Paleozóico Superior) no norte de Santa Catarina e sul do Paraná, Bacia do Paraná, Brasil. *Revista Brasileira de Geociências*, **40**(2):220-235.

Caputo M.V., Crowell J.C. 1985. Migration of glacial centers across Gondwana during Paleozoic Era. *The Geological Society of America Bulletin*, **96**:1020-1036.

Carvalho A.H., Vesely F.F. 2016. Facies relationships recorded in a Late Paleozoic fluvio-deltaic system (Paraná Basin, Brazil): Insights into the timing and triggers of subaqueous sediment gravity flows. *Sedimentary Geology*, **352**:45-62.

Carvalho P.F. 1940. Estrias glaciais em granodiorito sobposto ao Gondwana de Santa Catarina. *Mineração e Metalurgia*, **4**:271-272.

Castro L.G., Ferreira F.J.F., Cury L.F., Fiori A.P., Soares P.C., Lopes A.P., Oliveira M.J. 2014. Interpretação qualitativa e semiquantitativa dos dados aeromagnéticos sobre a Zona de Cisalhamento Lancinha, porção meridional do Cinturão Ribeira no Estado do Paraná, Sul do Brasil. Geologia USP, Série Científica, **14**(4):3-18.

Chen B., Joachimski M.M., Wang X., Shen S., Qi Y., Qie W. 2016. Ice volume and paleoclimate history of the Late Paleozoic Ice Age from conodont apatite oxygen isotopes from Naqing (Guizhou, China). *Palaeogeography, Palaeoclimatology, Palaeoecology*, **448**:151-161.

Chumakov N.M. 1981. Upper proterozoic glaciogenic rocks and their stratigraphic significance. *Precambrian Research*, **15**:373-395.

Clark C.D., Stokes C.R. 2005. Palaeo-ice stream landystem. *In*: Evans D.J.A. (Ed.) Glacial landsystems. Hodder Arnold, Oxford, pp. 204-227.

Cohen K.M., Finney S.C., Gibbard P.L., Fan J.X. 2013. The ICS International Chronostratigraphic Chart. *Episodes*, **36**:199-204.

Colgan P.M., Mickelson D.M. 1997. Genesis of streamlined landforms and flow history of the Green Bay Lobe, Wisconsin, USA. *Sedimentary Geology*, **111**(1-4):7-25.

Croot D.G. 1987. Glacio-tectonic structures: a mesoscale model of thin-skinned thrust sheets? *Journal of Structural Geology*, **9**(7):797-808.

Crowell J.C. 1999. Pre-Mesozoic Ice Ages: Their Bearing on Understanding the Climate System. *Geological Society of America Memoirs*, **192**:1-112.

d'Ávila R.S.F. 2009. Sequências deposicionais do Grupo Itararé (Carbonífero e Eopermiano), Bacia do Paraná, na área de Doutor Pedrinho e cercanias, Santa Catarina: turbiditos, pelitos e depósitos caóticos. Tese de Doutorado, Universidade do Vale do Rio dos Sinos, 233p.

Darvill C.M., Stokes C.R., Bentley M.J., Evans D.J.A., Lovell H. 2017. Dynamics of former ice lobes of the southernmost Patagonian Ice Sheet based on a glacial landsystems approach. *Journal of Quaternary Science*, **32**(6):857-876.

Di Pasquo M., Martínez M.A., Freije H. 2008. Primer registro palinológico de la Formación Sauce Grande (Pennsylvaniano-Cisuraliano) en las Sierras Australes, província de Buenos Aires, Argentina. *Ameghiniana,* **45**(1):69-81.

Dowdeswell J.A., Hogan K.A., Arnold N.S., Mugford R.I., Wells M., Hirst J.P.P, Decalf C. 2015. Sediment-rich meltwater plumes and ice-proximal fans at the margins of modern and ancient tidewater glaciers: Observations and modelling, **62**(6):1665-1692.

Dowdeswell J.A., Whittington R.J., Marienfield P. 1994. The origin of massive diamicton facies by iceberg rafting and scouring, Scoresby Sund, East Greenland. *Sedimentology*, **41**:21-35.

Dowdeswell J.A., Whittington R.J., Jennings A.E., Andrews J.T., Mackensen A., Marienfield P. 2000. An origin for laminated glacimarine sediments through sea-ice build-up and suppressed iceberg rafting. *Sedimentology*, **47**:557-576.

Du Toit A.L. 1927. A Geological Comparison of South America with South Africa. Carnegie Institution of Washington, Publication 381, 157p.

Dykstra M., Garyfalou K., Kertznus V., Kneller B., Milana J.P., Molinaro M., Szuman M., Thompson P. 2011. Mass-transport deposits: combining outcrop studies and seismic forward modeling to understand lithofacies distributions, deformation, and their seismic stratigraphic expression. *In*: Shipp R.C., Weimer P., Posamentier H.W. (Eds.) Mass-Transport Deposits in Deepwater Settings, 96, SEPM, Tulsa, pp. 423-454.

Ehlers J., Gibbard P.L. 2007. The extent and chronology of Cenozoic Global Glaciation. *Quaternary International*, **164**-**165**:6-20.

Evans D.J.A. 2005. Introduction to glacial landsystems. *In*: Evans D.J.A. (Ed.) Glacial Landsystems. Hodder Arnold, Oxford University Press, 1-11p.

Evans D.J.A., Clark C.D., Rea. B.R. 2008. Landform and sediment imprints of fast glacier flow in southwest Laurentide Ice Sheet. *Journal of Quaternary Science,* **23**(3):249-272.

Evans D.J.A., Lemmen D.S., Rea B.R. 1999. Glacial landsystems of the southwest Laurentide Ice Sheet: modern Icelandic analogues. *Journal of Quaternary Science*, **14**(7):673-691.

Evans D.J.A., Phillips E.R., Hiemstra J.F., Auton C.A., 2006. Subglacial till: formation, sedimentary characteristics and classification. *Earth-Science Reviews* **78**:115–176.

Eyles C.H., Eyles N., Miall A.D. 1985. Models of glaciomarine sedimentation and their application to the interpretation of ancient glacial sequences. *Palaeogeography, Palaeoclimatology, Palaeoecology*, **51**:15-84.

Eyles C.H., Lagoe M.B. 1990. Sedimentation patterns and facies geometries on a temperate glacially-influenced continental shelf: the Yakataga Formation, Middleton Island, Alaska. *In*: Dowdeswell J.A., Scourse J.D. (Eds.) Glacimarine Environments: Processes and Sediments. Geological Society Special Publication, 53, pp. 363-386.

Eyles N., Eyles C.H., Woodworth-Lynas C.M.T., Randall T.A. 2005. The sedimentary record of drifting ice (early Wisconsin Sunybrook deposit) in an ancestral icedammed Lake Ontario, Canada. *Quaternary Research,* **63**:171-181.

Fallgatter C., Paim P.S.G. 2017. On the origin of the Itararé Group basal nonconformity and its implications for the Late Paleozoic glaciation in the Paraná Basin, Brazil. *Palaeogeography, Palaeoclimatology, Palaeoecology,* (in press).

Fielding C.R., Frank T.D., Isbell J.L. 2008. The late Paleozoic ice age - a review of current understanding and synthesis of global climate patterns. *In*: Fielding C.R., Frank T.D., Isbell J.L. (Eds.) Resolving the Late Paleozoic Ice Age in Time and Space. Geological Society of America Special Paper, 441, pp. 343-354.

Fitzsimons S. Howarth J. 2018. Glaciolacustrine processes. *In:* Menzies J., van der Meer J. (Eds.) *Past Glacial Environments,* Elsevier, pp 309-334.

Fleming E.J., Benn D.I., Stevenson C.T.E., Petronis M.S., Hambrey M.J., Fairchild I.J. 2016. Glacitectonism, subglacial and glaciolacustrine processes during a Neoproterozoic panglaciation, sorth-east Svalbard. *Sedimentology*, **63**:411-442.

Flint R.F. 1957. *Glacial and the Pleistocene Geology*. John Wiley & Sons Inc., New York, 533p.

Fúlfaro V.J. 1996. Geología del Paraguay Oriental. *In:* Comin-Chiaramonti P., Gomes C.B. (Eds.) *Magmatismo alcalino en Paraguay Central-Oriental: Relaciones con Magmatismo coeval en Brasil*, Edusp/Fapesp, São Paulo, pp. 17-29.

Frakes L.A. 1979. *Climates throughout geologic time*. Elsevier, Amsterdan, 310p.

Frakes L.A., Crowell J.C. 1970. Late Paleozoic Glaciation: II, Africa Exclusive of the Karroo Basin. *Geological Society of America Bulletin*, **81**:2261-2286.

Frakes L.A., Francis J.E. 1988. A guide to Phanerozoic cold polar climates from high-latitude ice-rafting in the Cretaceous. *Nature*, **333**:547-549.

França A.B., Potter P.E. 1988. Estratigrafia, ambiente deposicional e análise de reservatório do Grupo Itararé (Permocarbonífero), Bacia do Paraná (parte 1). *Boletim de Geociências da Petrobrás*, **2**:147-191.

França A.B., Winter W.R., Assine M.L. 1996. Arenitos Lapa-Vila Velha: um modelo de trato de sistemas subaquosos canal-lobos sob influência glacial, Grupo Itararé (C-P), Bacia do Paraná. *Revista Brasileira de Geociências,* **26**(1):43-56.

Fuck R.A. 1966. Nota explicativa da folha geológica de Quero-Quero. *Boletim da Universidade Federal do Paraná, Geologia,* **19**,1-21.

Gesicki A.L.D., Riccomini C., Boggiani P.C. 2002. Ice flow during late Paleozoic glaciation in western Parana Basin, Brazil. *Journal of South American Earth Sciences*, **14**:933-939.

Glasser N.F., Jansson K.N., Harrison S., Kleman J. 2008. The glacial geomorphology and Pleistocene history of South America between 38°S and 56°S. *Quaternary Science Reviews,* **27**:365-390.

González-Bonorino G., Eyles N. 1995. Inverse relation between ice extent and the late Paleozoic glacial record of Gondwana. *Geology*, **23**(11):1015-1018.

Griffis N.P., Montañez I.P., Fedorchuck N., Isbell J., Mundil R., Vesely F., Weinshultz L., Ianuzzi R., Gulbanson R., Taboada A., Pagani A., Sanborn M.E., Huyskens M., Wimpenny J., Linol B., Yin Q.Z. 2018a. Isotopes to ice: Constraining provenance of glacial deposits and ice centers in west-central Gondwana. *Palaeogeography, Palaeoclimatology, Palaeoecology,* (aceito para publicação).

Griffis N.P., Mundil R., Montañez I.P., Isbell J., Fedorchuk N., Vesely F., Ianuzzi R., Yin Q.Z. 2018b. A new stratigraphic framework built on U-Pb single-zircon TIMS ages and implications for the timing of the penultimate icehouse (Paraná Basin, Brazil). *Geological Society of America Bulletin,* **130**(5-6):848-858.

Hambrey M.J. 1985. The late Ordovician-Early Silurian glacial period. *Palaeogeography, Palaeoclimatology, Palaeoecology*, **51**:273-289.

Hambrey M.J., Glasser N.F. 2012. Discriminating glacier thermal and dynamic regimes in the sedimentary record. *Sedimentary Geology*, **251**-**252**:1:33.

Hart J.K. 1995. Subglacial erosion, deposition and deformation associated with deformable beds. *Progress in Physical Geography*, **19**(2):173-191.

Hart J.K., Roberts D.H. 1994. Criteria to distinguish between subglacial glaciotectonic and glaciomarine sedimentation, I. Deformation styles and sedimentology. *Sedimentary Geology*, **91**:191-213.

Hart J.K., Boulton G.S. 1991. The interrelation of glaciotectonic and glaciodepositional processes within the glacial environment. *Quaternary Science Reviews*, **10**:335-350.

Hart J.K., Watts R.J. 1997. A comparison of the styles of deformation associated with two recent push moraines, south Van Keulenfjorden, Svalbard. *Earth Surface Processes and Landforms*, **22**:1089-1107.

Hart J.K., Hindmarsh R.C.A., Boulton G.S. 1990. Styles of subglacial glaciotectonic deformation within the context of the Anglian Ice-sheet. *Earth surface processes and landforms*, **15**:227-241.

Henriksen M., Mangerud J., Maslenikova O., Matiouchkov A., Tveranger J. 2001. Weichselian stratigraphy and glaciotectonic deformation along the lower Pechora River, Arctic Russia. *Global and Planetary Change,* **31**:297-319.

Henry C.L., Isbell J.L., Fielding C.R., Domack E.W., Frank T.D., Fraiser M.L., 2012. Proglacial deposition and deformation in the Upper Carboniferous to Lower Permian Wynyard Formation, Tasmania: A process analysis. *Palaeogeography, Palaeoclimatology, Palaeoecology*, **315**-**316**:142-157.

Holz M., França A.B., Souza P.A., Ianuzzi R., Rohn R. 2010. A stratigraphic chart of the late Carboniferous/Permian succession of the eastern border of the Paraná Basin, Brazil, South America. *Journal of South American Earth Sciences*, **29**:81-399.

Hornung J.J., Asprion U., Winsemann J. 2007. Jet-efflux deposits of a subaqueous ice-contact fan, glacial Lake Rinteln, northwestern Germany. *Sedimentary Geology*, **193**:167-192.

Huddart D., Hambrey M.J. 1996. Sedimentary and tectonic development of a high-arctic, thrust-moraine complex: Comfortlessbreen, Svalbard. *Boreas,* **25**:227-243.

Hunter L.E., Powell R.D., Lawson D.E. 1996. Flux of debris transported by ice at three Alaskan tidewater glaciers, *Journal of Glaciology*, **42**:123-135.

Ingólfsson O. 1987. The Late Wichselian glacial geology of the Melabakkar-Ásbakkar coastal cliffs, Borgarfördur, W-Iceland. *Jökull,* **37**:57-80.

Isbell J.L. 2010. Environmental and paleogeographic implications of glaciotectonic deformation of glaciomarine deposits within Permian strata of the Metschel Tillite, southern Victoria Land, Antarctica. *In*: López-Gamundí O.R., Buatois L.A. (Eds.), Late Paleozoic Glacial Events and Postglacial Transgressions in Gondwana, Geological Society of America Special Paper, 468, pp. 81–100.

Isbell J.L., Henry L.C., Gulbranson E.L., Limarino C.O., Fraiser M.L., Koch Z.J., Ciccioli P.L., Dineen A.A. 2012. Glacial paradoxes during the late Paleozoic ice age: Evaluating the equilibrium line altitude as control on glaciation. *Gondwana Research*, **22**:1-19.

Isbell J.L., Miller M.F., Wolfe K.L., Lenaker P.A. 2003. Timing of Paleozoic glaciation in Gondwana: Was glaciation responsible for the development of northern hemisphere cyclothems? *In:* Chan M.A., Archer A.W. (Eds.) Extreme depositional environments: mega end members in Geologic Time. *Geological Society of America Special Paper,* 370, pp. 5-24.

Kehew A.E., Esch J.M., Kozlowski A.L., Ewald S.K. 2012. Glacial landsystems and dynamics of the Saginaw Lobe of the Laurentide Ice Sheet, Michigan, USA. *Quaternary International,* **260**:21-31.

Kipper F. 2014. Palinoestratigrafia da porção inferior do Grupo Itararé (Carbonífero) no sudeste do estado do Paraná. Dissertação de Mestrado, Universidade Federal do Paraná.

Kipper F., Souza P.A., Vesely F.F. Palinomorfos e associações de fácies da Formação Lagoa Azul (Grupo Itararé, Pennsilvaniano da Bacia do Paraná) no sudeste do Estado do Paraná, Brasil. *Pesquisa em Geociências*, **44**(1):93-108.

Kjaer K.H., Korsgaard N.J., Schomacker A. 2008. Impact of multiple glacier surges: a geomorphological map from Brúarjökull, East Iceland. *Journal of Maps*, **4**:5-20.

Kluiving S.J. 1994. Glaciotectonics of the Itterbeck – Uelsen push moraines, Germany. *Journal of Quaternary Science*, **9**(3):235-244.

Koch Z.J., Isbell J.L. 2013. Processes and products of grounding-line fans from the Permian Pagoda Formation, Antarctica: Insight into glacigenic conditions in Gondwana. *Gondwana Research,* **24**:161-172.

Le Heron D.P. 2017. An exhumed Paleozoic glacial landscape in Chad. *Geology,* **46**(1):91-94.

Le Heron D.P., Craig J., Etienne J.L. 2009. Ancient glaciations and hydrocarbon accumulations in North Africa and the Middle East. *Earth-Science Reviews*, **93**:47-76.

Limarino C.O., Césari S.N., Spaletti L.A., Taboada A.C., Isbell J.L., Geuna S., Gulbranson E.L. 2014. A paleoclimatic review of southern South America during the late Paleozoic: A record from icehouse to extreme greenhouse conditions. *Gondwana Research*, **25**:1396-1421.

Lindsey D.A. 1971. Glacial marine sediments in the precambrian Gowganda formation at Whitefish Falls, Ontario (Canada). *Palaeogeography, Palaeoclimatology, Palaeoecology*, 9:7-25.

Lønne I. 1995. Sedimentary facies and depositional architecture of ice-contact glaciomarine systems. *Sedimentary Geology,* **98**:13-43.

Lønne I., Nemec W., Blikra L.H., Lauritsen T. 2001. Sedimentary architecture and dynamic stratigraphy of a marine ice-contact system. *Journal of Sedimentary Research*, **71**(6):922-943.

López-Gamundí O.R., Rossello E.A. 1993. Devonian-Carboniferous unconformity in Argentina and its relation to the Eo-Hercynian orogeny in southern South America. *Geologische Rundschau*, **82**(1):136-147.

López-Gamundí O.R., Rossello E.A. 1998. Basin fill Evolution and paleotectonic patterns along the Samfrau geosyncline: the Sauce Grande basin-Ventana fold belt (Argentina) and Karoo basin-Cape fold belt (South Africa) revisited. *Geologische Rundschau,* **86**:819-834.

Martin H. 1981. The Late Palaeozoic Dwyka Group of the South Kalahari Basin in Namibia and Botswana and the subglacial valleys of the Kaokoveld in Namibia. *In:* Hambrey M.J., Harland W.B. (Eds.) Earth's Pre-Pleistocene Glacial Record, pp. 61-66.

Martinsen O. 1994. Mass movements. *In*: Maltman A. (Ed.) The Geological Deformation of Sediments, Chapman & Hall, London, pp. 127–165.

McCabe A.M., Eyles N. 1988. Sedimentology of an ice-contact glaciomarine delta, Carey Valley, Northern Ireland. *Sedimentary Geology*, **59**:1-14.

McCarroll D., Rijsdijk K.F. 2003. Deformation styles as a key for interpreting glacial deposition environments. *Journal of Quaternary Science*, **18**(6):473-489.

Menzies J., van der Meer J.J.M., Shilts W.W. 2018. Subglacial processes and landforms. *In:* Menzies J., van der Meer J. (Eds.) *Past Glacial Environments,* Elsevier, pp. 105-158.

Milani E.J., de Wit M.J. 2008. Correlations between the classic Paraná and Cape-Karoo sequences of South America and southern Africa and their basin infills flaking the Gondwanides: du Toit revisited. *In:* Pankhurst R.J., Trouw R.A.J., Brito Neves B.B., de Wit M.J. (Eds) West Gondwana: Pre-Cenozoic Correlations Across the South Atlantic Region. Geological Society, London, Special Publications, 294, 319–342.

Milani E.J., Ramos V.A. 1998. Orogenias paleozoicas no domínio sul-ocidental do Gondwana e os ciclos de subsidência na Bacia do Paraná. *Revista Brasileira de Geociências,* **28**(4):473-484.

Miller J.M.G. 1996. Glacial Sediments. *In*: Reading H.G. (Ed.) Sedimentary Environments: Processes, Facies and Stratigraphy. Blackwell Science, Oxford, pp. 454-484.

Molnia B.F. 1983. Subartic glacial-marine sedimentation: a model. *In*: Molnia B.F. (Ed.) Glacial-marine sedimentation. Plenum Press, New York, pp 95-144.

Molnia B.F. 1989. Subartic (Temperate) Glacial-Marine sedimentation, The Northeast Gulft of Alaska. *In:* Anderson J.B., Molnia B.F. (Eds.) Glacial-Marine Sedimentation, 28th International Geological Congress, Washington, Short Course in Geology, 9, pp. 59-106.

Mottin T.E., Vesely F.F., Rodrigues M.C.N.L., Kipper F., Souza P.A., 2018. The paths and timing of late Paleozoic ice revisited: New stratigraphic and paleo-ice flow interpretations from a glacial succession in the upper Itararé Group (Paraná Basin, Brazil). *Palaeogeography, Palaeoclimatology, Palaeoecology,* **490**:488-504.

Mulder T., Alexander J. 2001. The physical character of subaqueous sedimentary density flows and their deposits. *Sedimentology*, **48**:269-299.

Muratori A. 1966. Nota explicativa da folha geológica de Campo Largo. *Boletim da Universidade Federal do Paraná, Geologia,* **21**:1-33.

Murray T. 1994. Glacial deformation. *In*: Maltman A. (Ed.) The Geological Deformation of Sediments, Chapman & Hall, London, pp. 73-93.

Nemec W. 1990. Aspects of sediment movement on steep delta slopes. *In*: Colella A., Prior D.B. (Eds.) Coarse-grained deltas. International Association of Sedimentologists, Special Publications, 10, pp. 29-73.

Ottesen D., Stokes C.R., Bøe R., Rise L., Longva O., Thorsnes T., Olesen O., Bugge T., Lepland A., Hestvik O.B. 2016. Landform assemblages and sedimentary processes along the Norwegian Channel Ice Stream, *Sedimentary Geology*, **338**:115-137.

Patterson C.J. 1997. Southern Laurentide ice lobes were created by ice streams: Des Moines Lobe in Minnesota, USA. *Sedimentary Geology*, **111**:249-261.

Patterson C.J. 1998. Laurentide glacial landscapes: The role of ice streams. *Geology*, **26**(7):643-646.

Pérez-Aguilar A., Petri S., Hypólito R., Ezaki S., Souza P.A. de, Juliani C., Monteiro L.V.S., Moschini F.A. 2009. Superfícies estriadas no embasamento granítico e vestígio de pavimento de clastos neopaleozoicos na região de Salto, SP. *Revista Escola de Minas,* 62:17-22.

Pfirman S.L., Solheim A. 1989. Subglacial meltwater discharge in the open-marine tidewater glacier environment: Observations from Nordaustlandet, Svalbard Archipelago. *Marine Geology*, **86**:265 281.

Phillips E.R. 2018. Glacitectonics. *In:* Menzies J., van der Meer J. (Eds.) *Past Glacial Environments,* Elsevier, pp 467-502.

Powell C.M., Li Z.X. 1994. Reconstruction of the Panthalassanmargin of Gondwanaland. *In*: Veevers J., Powell C. (Eds.) Permian–Triassic Pangea Basins and Foldbelts Along the Panthalassan Margin of Gondwanaland. Geologic Society of America Memoir, 184, pp. 5–9.

Powell R.D. 1981. A model for sedimentation by tidewater glaciers. *Annals of Glaciology*, **2:**129-134.

Powell R.D. 1990. Glacimarine processes at grounding-line fans and their growth to ice-contact deltas. *In*: Dowdeswell, J.A., Scourse, J.D. (Eds.) Glacimarine Environments: Processes and Sediments. Geological Society Special Publication, 53, pp. 53-73.

Powell R.D. 1994. Glacimarine processes and inductive lithofacies modelling of ice shelf and tidewater glacier sediments based on Quaternary examples. *Marine Geology,* **57**:1-52.

Powell R.D., Alley R.B. 1997. Grounding-line systems: processes, glaciological inferences and the stratigraphic record. *In*: Barker P.F., Cooper A.K. (Eds.) Geology and Seismic Stratigraphy of the Antarctic Margin, part 2, Anctartic Research Series, 71, American Geophysical Union, pp. 169-187.

Powell R.D., Domack E. 2002. Modern glaciomarine environments. *In*: Menzies J. (Ed.) Modern & Past glacial environments. Butterworth Heinemann, Oxford, pp. 361-390.

Powell R.D., Molnia B.F. 1989. Glacimarine sedimentary processes, facies and morphology of the south-southeast Alaska Shelf and fjords. *Marine Geology*, **85**:359-390.

Puigdomenech C.G., Carvalho B., Paim P.S.G., Faccini U.F. 2014. Lowstand turbidites and delta systems of the Itararé Group in the Vidal Ramos region (SC), southern Brazil. *Brazilian Journal of Geology*, **44**:529-544.

Rijsdijk K.F., Owen G., Warren W.P., McCaroll D., van der Meer J.J.M. 1999. Clastic dykes in over-consolidated tills: evidence for subglacial hydrofracturing at Killiney Bay, eastern Ireland. *Sedimentary Geology*, **129**:111-126.

Rijsdijk K.F., Warren W.P., van der Meer J.J.M. 2010. The glacial sequence at Killiney, SE Ireland: terrestrial deglaciation and polyphase glacitectonic deformation. *Quaternary Science Reviews,* **29**:696-719.

Rocha-Campos A.C., Farjallat J.E., Yoshida R. 1968. New glacial features of the Upper Paleozoic Itararé Subgroup in the State of São Paulo, Brazil. *Boletim da Sociedade Brasileira de Geologia,* 17:47-57.

Rocha-Campos A.C., Canuto J.R., Santos P.R., 2000. Late Paleozoic glaciotectonic structures in northern Paraná Basin, Brazil. *Sedimentary Geology*, **130**:131-143.

Rocha-Campos A.C., Oliveira M.E.C.B., Santos P.R., Saad A.R. 1976. Boulder pavements and the sense of movement of Late Paleozoic glaciers in central eastern of São Paulo state, Paraná, Brazil. *Boletim IG-USP*, **7**:149-160.

Rocha-Campos A.C., Santos P.R. 1981. The Itararé Subgroup, Aquidauana Group and San Gregório Formation, Paraná Basin, southeastern South America. *In: In:* Hambrey M.J., Harland W.B. (Eds.) Earth's Pre-Pleistocene Glacial Record, pp. 842-852.

Russell H.A.J., Arnott R.W.C. 2003. Hydraulic-jump and hyperconcentrated-flow deposits of a glacigenic subaqueous fan: Oak Ridge moraine, southern Ontario, Canada. **73**(6):887-905.

Rosa E.L.M., Vesely F.F., França A.B. 2016. A review on late Paleozoic ice-related landforms in the Paraná Basin: origin and paleogeographical implications. *Brazilian Journal of Geology*, **46**:147-166.

Sadowski G.R. 1991. A megafalha de Cubatão no sudeste brasileiro. *Boletim IG-USP Série Científica*, **22**:15-18.

Santos P.R. 1987. Fácies e evolução paleogeográfica do Subgrupo Itararé/Grupo Aquidauana (Neopaleozóico) na Bacia do Paraná, Brasil. Tese de Doutorado, Instituto de Geociências, Universidade de São Paulo, São Paulo, pp. 128.

Santos P.R. dos, Rocha-Campos A.C., Canuto J.R. 1992. Estruturas de arrasto de icebergs em ritmito do Subgrupo Itararé (Neopaleozoico), Trombudo Central, SC. *Boletim IG-USP,* **23**:1-18.

Santos P.R., Rocha-Campos A.C., Canuto J.R. 1996. Patterns of late Paleozoic deglaciation in the Parana Basin, Brazil. *Palaeogeography, Palaeoclimatology, Palaeoecology*, **125**:165-184.

Schneider R.L., Muhlmann H., Tommasi E., Medeiros R.A., Daemon R.A., Nogueira A.A. 1974. Revisão estratigráfica da Bacia do Paraná. *In:* 28º Congresso Brasileiro de Geologia, Porto Alegre, Anais, 1, pp. 41-65.

Sen D.P. 1980. Bedform, facies and basin model of anciel glacial deposit: a study based on Talchir (upper Carboniferous) rocks of Taratanr, Bihar, India. Palaeogeography, Palaeoclimatology, Palaeoecology, **32**:45-67.

Smith L.M., Andrews J.T. 2000. Sediment characteristics in iceberg dominated fjords, Kangerlussuaq region, East Greenland. *Sedimentary Geology*, **130**:11-25.

Souza P.A. 2006. Late Carboniferous palynostratigraphy of the Itararé Subgroup, northeastern Paraná Basin, Brazil. *Review of Palaeobotany and Palynology,* **138**:9-29.

Starck D., Gallardo E., Schulz A. 1993. The pre-Carboniferous unconformity in the Argentine portion of the Tarija basin. *In:* XII International Congress on Carboniferous-Permian, 2, *Comptes Rendus*, p. 373-384.

Stow D.A., Shanmugan G. 1980. Sequence of structures in fine-grained turbidites: comparison of recent deep-sea and ancient flysch sediments. *Sedimentary Geology*, **25**: 23-42.

Streuff K., Ó Cofaigh C., Noormets R., Lloyd J. 2017. Submarine landform assemblages and sedimentary processes in front of Spitsbergen tidewater glaciers. *Marine Geology,* (em impressão).

Strugale M., Rostirolla S.P., Mancini F., Portela Filho C.V., Ferreira F.J.F., Freitas R.C. 2007. Structural framework and Mesozoic-Cenozoic evolution of Ponta Grossa Arch, Paraná Basin, southern Brazil. *Journal of South American Earth Sciences*, **24**:203-227.

Sturm M., Matter A. 1978. Turbidites and varves in Lake Brienz (Switzerland): Deposition of clast detritus by density currents. *In:* Matter A., Tucker M.E. (Eds.) Modern and Ancient Lake Sediments, The International Association of Sedimentologists, pp 147-168.

Syverson K.M., Colgan P.M. 2004. The Quaternary of Wisconsin: a review of stratigraphy and glaciation history. *In*: Ehlers J., Gibbard P.L. (Eds.) Quaternary Glaciations – Extent and Chronology, Part II: North America. Elsevier Publishing, Amsterdan, pp. 295-311.

Thomas G.S.P., Connell R.J. Iceberg drop, dump and grounding structures from Pleistocene glacio-lacustrine sediments, Scotland. *Journal of Sedimentary Petrology,* **55**(2):243-249.

Tomazelli L.J, Soliani E. 1982. Evidências de atividade glacial no Paleozoico Superior do Rio Grande do Sul. *In*: 32° Congresso Brasileiro de Geologia, Salvador, Anais, 4, pp. 1378-1391.

Tomazelli L.J. & Soliani E. 1997. Sedimentary Facies and Depositional Environments Related to Gondwana Glaciation in Batovi and Suspiro Regions, Rio Grande do Sul, Brazil. *Journal of South American Earth Sciences*, **10**:295-303.

Trosdtorf I., Assine M.L., Vesely F.F., Rocha-Campos A.C., Santos P.R., Tomio A., 2005. Glacially striated, soft sediment surfaces on late Paleozoic tillite at São Luiz do Purunã, PR. *Anais da Academia Brasileira de Ciências*, **77**:367–378.

Urban B., Bigga G. 2015. Environmental reconstruction and biostratigraphy of late Middle Pleistocene lakeshore deposits at Schöningen. *Journal of Human Evolution*, **89**:57-70.

van der Meer J.J.M., Menzies J., Rose J. 2003. Subglacial till: the deforming glacier bed. *Quaternary Science Reviews*, **22**:1659–1685.

van der Wateren F.M. 1985. A model of glacial tectonics, applied to the ice-pushed ridges in Central Netherlands. *Bulletin of the Geological Society of Denmark,* **34**:55-74.

van der Wateren F.M. 1994. Proglacial subaquatic outwash fan and delta sediments in push moraines – indicators of subglacial meltwater activity. *Sedimentary Geology*, **91**:145-172.

van der Wateren F.M. 1995. Structural Geology and Sedimentology of Push Moraines. *Mededelingen Rijks Geologische Dienst*, **54**:1-168.

van der Wateren F.M. 2002. Processes of glaciotectonism. *In*: Menzies J. (Ed.) Modern & Past glacial environments. Butterworth Heinemann, Oxford, pp. 417-444.

Veevers J.J., Powell M. 1987. Late Paleozoic glacial episodes in Gondwanaland reflected in transgressive-regressive depositional sequences in Euramerica. *Geological Society of America Bulletin*, **98**:475-487.

Vesely F.F. & Assine M.L. 2004. Sequências e tratos de sistemas deposicionais do Grupo Itararé, norte do estado do Paraná. *Revista Brasileira de Geociências*, **34**:219-230.

Vesely F.F., Assine M.L. 2006. Deglaciation sequences in the Permo-Carboniferous Itararé Group Paraná Basin, southern Brazil. *Journal of South American Earth Sciences*, **22**:56-168.

Vesely F.F., Assine M.L. 2014. Ice-keel scour marks in the geological record: evidence from carboniferous soft-sediment striated surfaces in the Paraná Basin, southern Brazil. *Journal of Sedimentary Research*, **84**:26-39.

Vesely F.F., Rodrigues M., Rosa E.L.M., Amato J., Trzaskos A., Isbell J., Fedorchuk N. 2018. Recurrent emplacement of non-glacial diamictite during the late Paleozoic ice age, *Geology* (aceito para publicação).

Vesely F.F., Trzaskos B., Kipper F., Assine M.L., Souza P.A. 2015. Sedimentary record of a fluctuating ice margin from the Pennsylvanian of western Gondwana: Paraná Basin, southern Brazil. *Sedimentary Geology*, **326**:45-63.

Vesely F.F., Trzaskos B., Mottin T.E., Rodrigues M.C.N.L., Schemiko D.C.B., Rosa E.L.M., Carvalho A.H., Kipper F., Souza P.A., Ianuzzi R., Paim P.S.G., Isbell J.L., Fedorchuk N.D., Montañez I.P., Griffs N.P., Mundil R. 2017. Late Paleozoic tectonics, glaciation and sedimentation in the Paraná Basin: lastest advances. *In*: X Simpósio Sul-Brasileiro de Geologia, Anais, Curitiba.

Visser J.N.J. 1987. The Paleogeography of Part of Southwestern Gondwana During the Permo-Carboniferous Glaciation. *Palaeogeography, Palaeoclimatology, Palaeoecology,* **61**:205-219.

Visser J.N.J. 1997. Deglaciation sequences in Permo-Carboniferous Karoo and Kalahari basins of southern Africa: a tool in the analysis of cyclic glaciomarine basin fills. *Sedimentology*, **44**:507-521.

Visser J.N.J., Colliston W.P., Terblanche J.C. 1984. The origin of soft-sediment deformation structures in Permo-Carboniferous glacial and proglacial beds, South Africa. *Journal of Sedimentary Petrology,* **54**(4):1183-1196.

Viviani J.B. & Rocha-Campos A.C. 2002. Late Paleozoic exhumed glacial erosive landscape in Salto, SP. *Anais da Academia Brasileira de Ciências,* 74:549-550.

Walker R.G. 1965. The origin and significance of the internal sedimentary structures of turbidites. *Proceedings of the Yorkshire Geological Society*, **35**(1):1-32.

White I.C. 1908. Relatório sobre as Coal Measures e rochas associadas no sul do Brasil. Comissão de Estudos das Minas de Carvão de Pedra, Rio de Janeiro, Relatório Final.

Woodworth-Lynas C.M.T., Dowdeswell J.D. 1994. Soft-sediment striated surfaces and massive diamicton facies produced by floating ice. *In:* Deynoux M., Miller J.M.J., Domack E.W., Eyles N., Fairchild I.J., Young G.M. (Eds.) Earth's Glacial Record. Cambridge University Press, pp. 241–259.

Young G.M., Von Brunn V. Gold D.J.C, Minter W.E.L. 1998. Earth's Oldest Reported Glaciation: Physical and Chemical Evidence From the Archean Mozaan Group (~2.9 Ga) of South Africa. *The Journal of Geology*, **106**:523-538.